

Reason is but choosing: On the alternatives for bath correlators and spectral densities from mixed quantum-classical simulations

Stéphanie Valteau¹, Alexander Eisfeld², and Alán Aspuru-Guzik^{1,*}

¹*Department of Chemistry and Chemical Biology, Harvard University, Cambridge, Massachusetts 02138, USA*

²*Max Planck Institute for the Physics of Complex Systems, Nöthnitzer Straße 38, 01187 Dresden, Germany*

We investigate on the procedure of extracting a “spectral density” from mixed QM/MM calculations and employing it in open quantum systems models. In particular, we study the connection between the energy gap correlation function extracted from ground state QM/MM and the bath spectral density used as input in open quantum system approaches. We introduce a simple model which can give intuition on when the ground state QM/MM propagation will give the correct energy gap. We also discuss the role of higher order correlators of the energy-gap fluctuations which can provide useful information on the bath. Further, various semiclassical corrections to the spectral density, are applied and investigated. Finally, we apply our considerations to the photosynthetic Fenna-Matthews-Olson complex. For this system, our results suggest the use of the Harmonic prefactor for the spectral density rather than the Standard one, which was employed in the simulations of the system carried out to date.

I. INTRODUCTION

In the study of the dynamics of large systems such as photosynthetic complexes, reduced models, which provide information on a small set of system degrees of freedom at the price of tracing out the rest of the bath degrees of freedom, have become very popular. Amongst these methods, which are open quantum systems approaches, one can find various quantum master equations [1–22] and Stochastic Schrödinger Equations [23, 24], which often rely on describing the system-bath interaction through a two-time “bath correlation function” or a “bath spectral density”. The reason for the quotes is that there is no unique way of obtaining these two quantities if one resorts to quasiclassical theories. In 1644, John Milton argued for the fact that “Reason is but choosing” [25], which inspires the philosophy behind this paper. Collecting information about the problem at hand may allow for better choices amongst the possible alternatives of the methods available to obtain these quantities.

As a case study, in the present work, we consider the Fenna-Matthews-Olson (FMO) light-harvesting pigment protein complex found in green sulfur bacteria. For this system, recent efforts have been undertaken to extract the bath spectral densities from mixed quantum-classical calculations [26–28]. The FMO complex has a trimeric structure, where each monomer contains, within the protein scaffolding, eight bacteriochlorophyll (BChl) molecules, which can transport electronic excitation energy. Up to recently, it was thought that only seven of the BChl’s actually were present and most of the previous studies have focused on that case. Shim’s results [27] which we employ in this work, are indeed based on the case of one monomer with seven BChl molecules. Experimentally, it has been possible to extract a spectral density which is an average over the BChls [29, 30]. However, one can expect that each BChl has a different spectral density, due to its specific protein environment.

A straightforward theoretical approach to obtain the spectral densities from a microscopic description is a mixed quantum mechanics/classical mechanics (QM/MM) model [31]. In this approach, the nuclear degrees of freedom are treated classically and the relevant system quantities are calculated quantum mechanically. Then, from the microscopic description, spectral densities and correlation functions can be extracted and employed in the reduced models.

A specific QM/MM approach, which has become popular in recent years in the context of photosynthetic complexes [26, 27, 32, 33] and has been employed for FMO [26, 27], consists in propagating the nuclei in the ground electronic state of the FMO complex, thus the change in the classical forces due to excitation of the BChls is ignored. The bath correlation function and spectral densities are then extracted from the energy gap trajectories, i.e. the electronic transition energies which depend on the time dependent nuclear configuration. This transition energy is calculated using quantum chemistry, for example TDFT [27] or semi-empirical approaches [26]. One thus obtains a time dependent energy gap two-time correlation function.

In this work, we shed light on the connection between the mixed QM/MM gap correlation function and the open quantum system bath correlation function using a simple model. The mixed QM/MM gap correlation function is real. However, in general, the full quantum correlation function will have an imaginary part. We employ different semiclassical *a posteriori* corrections to recover this part and compare the resulting spectral densities. Much work has been carried out on these *a posteriori* semiclassical corrections [34–39], but the question of which approximation is best remains open. Towards answering this question, we show that a simple model of shifted harmonic Born-Oppenheimer surfaces leads to two of the semiclassical *a posteriori* corrections, each obtained with a different phase space probability distribution. We thus establish the link to a microscopic picture. This model of shifted harmonic potential surfaces is of particular interest, since the spectral density used in the open quantum system approaches emerges from such a description.

Finally, we will investigate whether the results of the

* aspuru@chemistry.harvard.edu

QM/MM fulfill the requirements needed to employ the extracted spectral density in open quantum system methods. These methods rely on the validity of assumptions such as linear coupling of the system to the bath and a bath of harmonic oscillators. We attempt to investigate whether these assumptions are valid in our case by evaluating higher order correlators of the energy gap time traces. In addition, we compare the spectral densities obtained at different temperatures. In most open quantum system approaches, when the harmonic bath approximation is employed, the spectral density is temperature independent. Thus, one can use this invariance as a criteria for choosing which of the applied *a posteriori* corrections is most reasonable. In particular, our findings suggest that the best *a posteriori* semiclassical approximation for FMO is the Harmonic [40, 41] correction rather than the Standard [42–44] one, which has so far been employed in the context of the simulation of exciton dynamics in photosynthetic complexes [26–28, 33]. Together, these aspects provide a clearer microscopic picture of the complex approximations involved in combining ground state QM/MM and open quantum system approaches.

The paper is structured as follows: we begin by introducing the general quantum two-time correlation function in Section II. We introduce its time symmetries and its Fourier transform and subsequently we define the spectral density. A brief summary of the general *a posteriori* semiclassical approximations to the quantum Fourier transform of the correlator from the classical Fourier transform is given in Section II C. In Section III, we introduce the concept of an energy gap correlation function for two-level systems as models for molecules coupled to a bath and show how this leads to a quantum bath correlation function and spectral density which are consistent with the open quantum system approach. In Section IV, we show that one can introduce a microscopic model which leads to some of the same prefactors described in the general case in Section II C. Finally, we investigate the conditions of linear system-bath coupling and harmonic bath in Section V. In particular, we evaluate high-order multi-time correlation functions for the bath. These considerations are applied to our specific QM/MM calculations for FMO in Section VI. We conclude in Section VII by summarizing our findings.

II. THE QUANTUM CORRELATION FUNCTION AND THE SPECTRAL DENSITY

In this section, we introduce the definition of the quantum two-time bath correlation function. The generic Hamiltonian of a system coupled to a bath, in the absence of external fields, can be expressed as

$$\hat{H} = \hat{H}_S(\mathbf{q}, \mathbf{p}) + \hat{H}_B(\mathbf{Q}, \mathbf{P}) + \hat{H}_{SB}(\mathbf{q}, \mathbf{p}, \mathbf{Q}, \mathbf{P}), \quad (1)$$

where \hat{H}_S is the system Hamiltonian, \hat{H}_B is the bath Hamiltonian, \hat{H}_{SB} is the system-bath Hamiltonian. In addition, $(\mathbf{q}, \mathbf{p}) = (q_j, p_j)$ and $(\mathbf{Q}, \mathbf{P}) = (Q_k, P_k)$, indicate the generalized multidimensional conjugated coordinates for the system and the bath respectively. The indexes $j = 1, \dots, f$ and $k = 1, \dots, F$ run over the system (f) and bath (F) degrees

of freedom respectively. The system-bath Hamiltonian can be written as a function of the system, \hat{A} , and bath, \hat{B} , operators:

$$\hat{H}_{SB}(\mathbf{q}, \mathbf{p}, \mathbf{Q}, \mathbf{P}) = \sum_m \hat{A}_m(\mathbf{q}, \mathbf{p}) \otimes \hat{B}_m(\mathbf{Q}, \mathbf{P}). \quad (2)$$

The influence of the bath on the system can be described by time-correlation functions. We will mostly focus on the two-time bath correlation function VII, which is defined as

$$C_{nm}(t, t') = \text{tr}_B \{ \hat{B}_n(t, \mathbf{Q}, \mathbf{P}) \hat{B}_m(t', \mathbf{Q}, \mathbf{P}) \hat{\rho}_B \}. \quad (3)$$

Here, the time dependent bath operators are expressed as $\hat{B}_m(t, \mathbf{Q}, \mathbf{P}) = e^{i\hat{H}_B t/\hbar} \hat{B}_m(\mathbf{Q}, \mathbf{P}) e^{-i\hat{H}_B t/\hbar}$. If the bath density matrix $\hat{\rho}_B$ is a stationary state of the reservoir, i.e. $[\hat{H}_B, \hat{\rho}_B] = 0$, then the correlator will be homogeneous in time [45], and depend only on the difference in time $\tau = t - t'$, namely,

$$C_{nm}(t, t') = C_{nm}(\tau) = \text{tr}_B \{ \hat{B}_n(\tau, \mathbf{Q}, \mathbf{P}) \hat{B}_m(0, \mathbf{Q}, \mathbf{P}) \hat{\rho}_B \}. \quad (4)$$

In the following we will be interested only in the $n = m$ correlators, which we will indicate as $C(t)$, dropping the subscript notation for simplicity. Finally, we define the equilibrium bath density matrix operator

$$\hat{\rho}_B = \frac{e^{-\beta \hat{H}_B}}{\text{tr}_B \{ e^{-\beta \hat{H}_B} \}}, \quad (5)$$

where $\beta = 1/(k_B T)$ and T is the temperature. In section V, we will briefly discuss higher order correlators.

A. Fourier transform of the time correlation function and symmetries of the correlator

The correlator defined in the previous section is in general complex and one can show, see e.g. [42, 46], that it has the following symmetries with respect to time,

$$C(-t) = C^*(t) = C(t - i\beta\hbar). \quad (6)$$

These symmetries result from Eqs 4 and 5. In addition, by looking at the expansion of the Fourier transform of $C(t)$ with respect to \hbar and using its second time symmetry in Eq. 6, one sees [35, 47] that the real and imaginary parts of $C(t)$ are related by

$$\text{Im}\{C(t)\} = \tan\left(\frac{\beta\hbar}{2} \frac{d}{dt}\right) \text{Re}\{C(t)\}. \quad (7)$$

It is also useful to note that the real part of $C(t)$ is symmetric and the imaginary part is antisymmetric with respect to time. This connection is the starting point of many of the semiclassical approximations to the quantum correlation function as described in Appendix A.

We then define $G(\omega)$ the Fourier transform of the time correlation function

$$G(\omega) \equiv \mathcal{F}[C(t)](\omega) = \int_{-\infty}^{\infty} e^{i\omega t} C(t) dt. \quad (8)$$

The function $G(\omega)$ is in general, temperature dependent, real and positive. In this work, we will refer to it as the Temperature-Dependent Coupling Density (TDCD). It will be convenient to split $G(\omega)$ into a symmetric and antisymmetric component which originate respectively from the real and imaginary parts of $C(t)$,

$$G(\omega) = G_{\text{sym}}(\omega) + G_{\text{asym}}(\omega), \quad (9)$$

with

$$G_{\text{sym}}(\omega) = \frac{1}{2} (G(\omega) + G(-\omega)) \quad (10)$$

$$G_{\text{asym}}(\omega) = \frac{1}{2} (G(\omega) - G(-\omega)). \quad (11)$$

In the definitions Eq. 9-11 we have followed the convention of Ref. [35]. Note that in the literature there exist other definitions. E.g. the corresponding equations in Ref. [48], differ by a factor of 2 from the ones used here [49]. The detailed-balance condition, which follows directly from the second time symmetry in Eq. 6, implies that the overall TDCD is related to its symmetric part by

$$G(\omega) = \frac{2}{1 + e^{-\beta\hbar\omega}} G_{\text{sym}}(\omega), \quad (12)$$

$$= (1 - \coth(\beta\hbar\omega/2)) G_{\text{sym}}(\omega). \quad (13)$$

Alternatively, one can employ the asymmetric part to obtain,

$$G(\omega) = \frac{2}{1 - e^{-\beta\hbar\omega}} G_{\text{asym}}(\omega) \quad (14)$$

$$= (1 + \coth(\beta\hbar\omega/2)) G_{\text{asym}}(\omega). \quad (15)$$

We have expressed both equalities as a function of hyperbolic functions which will later be found in the various semiclassical expressions of $G(\omega)$.

B. The spectral density

Another quantity which is often of interest is the so-called “spectral density”. There are different definitions of spectral density in the literature. For later use in Section II C, we define the spectral density $j(\omega)$ as the positive frequency part of $G_{\text{asym}}(\omega)$ [50]

$$j(\omega) = G_{\text{asym}}(\omega) / (2\pi) ; \omega \geq 0. \quad (16)$$

The spectral density $j(\omega)$ describes the coupling of the system to the bath for a given frequency. We extend the spectral density $j(\omega)$ to negative frequencies by defining

$$J(\omega) \equiv G_{\text{asym}}(\omega) = \begin{cases} 2\pi \cdot j(\omega) & ; \omega \geq 0 \\ -2\pi \cdot j(-\omega) & ; \omega < 0 \end{cases}. \quad (17)$$

Using Eq. 14 and the definition of $G(\omega)$, Eq. 8, one can express the correlation function as a function of $G_{\text{asym}}(\omega)$,

$$C(t) = \frac{1}{2\pi} \int_{-\infty}^{\infty} d\omega e^{-i\omega t} (\coth(\beta\hbar\omega/2) + 1) J(\omega). \quad (18)$$

C. General semiclassical a posteriori approximations

For systems of more than a few degrees of freedom, and in general, it is difficult to calculate the exact correlation function, and therefore its Fourier transform, by using a fully quantum mechanical treatment. However, using classical mechanics one can obtain its classical counterpart with much less effort. Therefore, it is common to attempt to construct the quantum spectral density from the classical one.

Here, we define the fully-classical correlation function as the classical $\hbar \rightarrow 0$ limit of Eq. 3,

$$C^{\text{cl}}(t) = \int d\mathbf{Q} d\mathbf{P} B(t, \mathbf{Q}, \mathbf{P}) B(0, \mathbf{Q}, \mathbf{P}) \mathcal{W}(\mathbf{Q}, \mathbf{P}). \quad (19)$$

The classical bath phase-space density is defined as

$$\mathcal{W}(\mathbf{Q}, \mathbf{P}) = \frac{e^{-\beta H_{\text{B}}(\mathbf{Q}, \mathbf{P})}}{\int d\mathbf{Q} d\mathbf{P} e^{-\beta H_{\text{B}}(\mathbf{Q}, \mathbf{P})}}. \quad (20)$$

Here, the quantum bath operators \hat{B} in Eq. 3 have been substituted by classical functions of the phase space variables $B(t, \mathbf{Q}, \mathbf{P})$. Also, the bath density matrix is replaced by the normalized equilibrium classical bath Boltzmann distribution. The classical TDCD is defined as

$$G^{\text{cl}}(\omega) = \mathcal{F}[C^{\text{cl}}(t)](\omega) = \int_{-\infty}^{\infty} e^{i\omega t} C^{\text{cl}}(t) dt. \quad (21)$$

Note that $C^{\text{cl}}(t)$ is a real and symmetric function in contrast to its quantum counterpart. This is also the case of the mixed QM/MM simulations employed for FMO in [26, 27], in which the resulting correlation function is real and none of the imaginary part is recovered.

It is now desirable to be able re-construct, at least partially, the exact quantum spectral density from the classical one, through a simple description. Ideally, such a correction should be applied *a posteriori* and should not require extensive additional computation. Much work has been carried out in this direction, see e.g. [34–39]. As described in Ref. [35], one can define various semiclassical approximations to the full quantum mechanical $G(\omega)$ starting from its classical counterpart $G^{\text{cl}}(\omega)$. We report each of these approximations in Table I, second column, and a brief discussion can be found in Appendix A.

These corrections all originate from expansions in \hbar and use of the symmetry properties of the two-time correlation function and its Fourier transform. Note that if one expands the quantum correlator $C(t)$ in powers of \hbar , the first term is real and symmetric and corresponds to $C^{\text{cl}}(t)$. The assumption that $C(t) = C^{\text{cl}}(t)$, which leads to the standard approximation, is in general not correct. In fact, since both of the correlation functions are obtained after thermal averaging, we see that they must differ at least by their respective partition functions.

The specific functional form of each of these prefactors for $G(\omega)$, is plotted in Fig. 1 as a function of the temperature scaled frequency $\omega_{\text{b}} = \beta\hbar\omega$. We see that at low frequencies,

Table I. Column two: Various expressions for obtaining a semiclassical temperature-dependent coupling density TDCD $G(\omega)$ from the classical $G^{\text{cl}}(\omega)$ as discussed in, e.g. [35]. Column three: Expressions for obtaining the semiclassical asymmetric TDCD $J(\omega)$ from the classical $G^{\text{cl}}(\omega)$. These follow from the expressions in column two and from detailed balance (Eq. 14).

Method	Expression for $G(\omega)$	Expression for $J(\omega) = G_{\text{asym}}(\omega)$
Standard [42–44]	$G^{\text{std}}(\omega) = \frac{2}{1+e^{-\beta\hbar\omega}} G^{\text{cl}}(\omega)$	$J^{\text{std}}(\omega) = \tanh\left(\frac{\beta\hbar\omega}{2}\right) G^{\text{cl}}(\omega)$
Harmonic [40–42]	$G^{\text{harm}}(\omega) = \frac{\beta\hbar\omega}{1-e^{-\beta\hbar\omega}} G^{\text{cl}}(\omega)$	$J^{\text{harm}}(\omega) = \frac{\beta\hbar\omega}{2} G^{\text{cl}}(\omega)$
Schofield [51]	$G^{\text{scho}}(\omega) = e^{\beta\hbar\omega/2} G^{\text{cl}}(\omega)$	$J^{\text{scho}}(\omega) = \sinh\left(\frac{\beta\hbar\omega}{2}\right) G^{\text{cl}}(\omega)$
Egelstaff [52]	$G^{\text{egel}}(\omega) = e^{\beta\hbar\omega/2} \int_{-\infty}^{\infty} e^{i\omega t} C^{\text{cl}}\left(\sqrt{t^2 + (\beta\hbar/2)^2}\right) dt$	$J^{\text{egel}}(\omega) = \sinh\left(\frac{\beta\hbar\omega}{2}\right) \mathcal{F}\left[G^{\text{cl}}(\sqrt{t^2 + (\beta\hbar/2)^2})\right](\omega)$
Schofield-Harmonic [35]	$G^{\text{s-h}}(\omega) = e^{\beta\hbar\omega/4} \sqrt{\frac{\beta\hbar\omega}{1-e^{-\beta\hbar\omega}}} G^{\text{cl}}(\omega)$	$J^{\text{s-h}}(\omega) = \sqrt{\frac{\beta\hbar\omega}{2}} \sinh\left(\frac{\beta\hbar\omega}{2}\right) G^{\text{cl}}(\omega)$

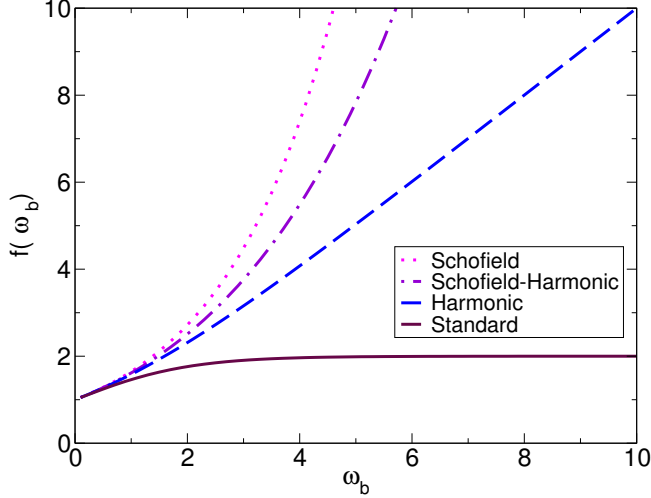


Figure 1. Prefactors for the temperature-dependent coupling density (TDCD) $G(\omega)$ (Tab. I, column two) plotted as a function of $\omega_b = \omega_b \hbar$. One sees that for $\hbar\omega/k_B T < 1$ they coincide. The prefactors for the asymmetric $J(\omega) = G^{\text{asym}}(\omega)$ (Tab. I, column three) follow the same trend with the difference that $J(0) = 0$.

$\omega_b < 1$ (i.e. $\hbar\omega < k_B T$) all approximations give nearly identical results and give the same value for $\omega_b = 0$.

The various approximations to the spectral density can straightforwardly be derived from those of $G(\omega)$ by using Eq. 14. The resulting expressions are reported in column three of Table I and the prefactors follow the same trend as those for $G(\omega)$ as a function of frequency.

Now, given all the functional forms described above, the question is how to reason and choose the most appropriate one. For the FMO complex, it is unclear at first sight which one would be the best. In Section IV, we will investigate a model to elucidate the origin of these prefactors. This will help to discriminate between these corrections. In Section VI, we will apply all of the corrections listed in Table I to our energy gap traces and discuss the differences between each approach.

III. ENERGY GAP CORRELATION FUNCTION FOR A SIMPLE MODEL

In the mixed QM/MM calculations for photosynthetic systems [26, 27, 33], the nuclear trajectories are propagated in the electronic ground state using MD with short time steps. For a set of longer times steps within these trajectories, the electronic transition energies of the BChl molecules are computed using an electronic structure calculation method. Because it is computationally costly to calculate the electronic states for the full set of seven/eight coupled BChls simultaneously [26], the system was divided into seven/eight subsystems for which the electronic states were calculated separately. Thus, in these calculations no excited state interactions are included explicitly [53]. The Hamiltonian of the coupled BChls is then written as $H = \sum_{n=1}^N H_n + \sum_{n < m} V_{nm}$ where H_n denotes the Hamiltonian of BChl n and V_{nm} is the Coloumb (transition dipole-dipole) interaction between them. To establish a connection to the open quantum system approach, each BChl is treated as an electronic two level system. These two-level systems and the electronic interaction between them are taken to be the system part. The coupling to internal nuclear degrees of freedom an the surrounding protein will then lead to fluctuations of these quantities in time (for more details see e.g. [33]). From the time dependence of the transition energy between electronic ground and excited state for each BChl, a classical ground-excited state energy-gap correlation function can be obtained. In turn, spectral densities can be extracted from the energy-gap correlation functions.

The gap correlation function, as obtained from the MD simulations, is a quantity which up to the previous section, has not been connected to the open quantum system approach described in Sec. II. To this end, in this Section, we will explore a simple model with Born-Oppenheimer (BO) surfaces which can clarify the connection.

A. Quantum correlation function and energy gap correlation function for a molecule

Lets us begin by considering a single molecule (BChl) treated in the Born-Oppenheimer approximation. The molecule is modeled as a two-level system with an electronic adiabatic ground $|g\rangle$ and excited $|e\rangle$ state. This situation is

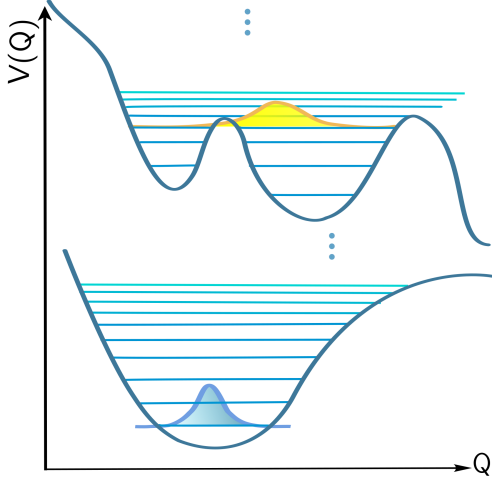


Figure 2. Sketch of two generic Born-Oppenheimer (BO) surfaces. This sketch indicates the model which we consider in Sec. III A to define the energy gap correlation function in the context of an arbitrary molecule.

depicted in Fig. 2. We can think of the BO-surfaces as having the dependence of the environment (protein and other BChls) already included, ignoring however the resonant dipole-dipole interaction. The approximation of two levels is reasonable in the limit where the next excited state is very far in energy space from the first. Usually, non-adiabatic couplings can be also neglected, as chosen in our calculations. Given this model, we investigate how the general correlation function, Eq. 3, is related to the energy gap correlation function.

We write the full Hamiltonian formally as

$$\hat{H} = \hat{H}_g(\mathbf{Q}, \mathbf{P}) |g\rangle\langle g| + \hat{H}_e(\mathbf{Q}, \mathbf{P}) |e\rangle\langle e|, \quad (22)$$

where $\hat{H}_g(\mathbf{Q})$ and $\hat{H}_e(\mathbf{Q})$ are the nuclear Hamiltonians for the ground and excited state in the BO approximation. In mass scaled coordinates $(Q_j = \sqrt{m_j} q_j; P_j = \frac{p_j}{\sqrt{m_j}})$ the Hamiltonians can be expressed as

$$\hat{H}_g(\mathbf{Q}, \mathbf{P}) = \sum_{j=1}^F \frac{P_j^2}{2} + V_g(\mathbf{Q})$$

and $\hat{H}_e(\mathbf{Q}, \mathbf{P}) = \hat{H}_g(\mathbf{Q}, \mathbf{P}) + \hat{\Delta}_{eg}(\mathbf{Q})$ where $V_g(\mathbf{Q})$ denotes the ground state potential energy surface. For later purpose, we have expressed the excited state nuclear Hamiltonian with respect to the ground state potential by introducing the energy gap operator,

$$\begin{aligned} \hat{\Delta}_{eg}(\mathbf{Q}) &= \hat{H}_e(\mathbf{Q}, \mathbf{P}) - \hat{H}_g(\mathbf{Q}, \mathbf{P}) \\ &= \hbar\omega_{eg} + \lambda_0 + V_e(\mathbf{Q}) - V_g(\mathbf{Q}). \end{aligned} \quad (23)$$

This operator quantifies the energy difference between the excited state and the ground state surface. A coordinate independent constant energy difference $\hbar\omega_{eg} + \lambda_0$ has been explicitly written down, so that the remaining part $V_e(\mathbf{Q}) - V_g(\mathbf{Q})$ does not contain any coordinate independent contributions. This notation and the division into two parts $\hbar\omega_{eg}$ and λ_0 will become clear later.

The total Hamiltonian can be rewritten as

$$\hat{H} = \hat{H}_g \cdot \hat{\mathbb{I}} + (\hbar\omega_{eg} + \lambda_0) |e\rangle\langle e| + \hat{\Delta} |e\rangle\langle e|, \quad (24)$$

where we have defined the *reduced* gap operator $\hat{\Delta} \equiv \hat{\Delta}_{eg} - \hbar\omega_{eg} - \lambda_0$.

To establish a connection to the open quantum system model, as presented in Sec. II, we choose

$$\hat{H}_B = \hat{H}_g(\mathbf{Q}, \mathbf{P}) \quad (25)$$

$$\hat{H}_{SB} = \hat{\Delta}(\mathbf{Q}) |e\rangle\langle e| \quad (26)$$

$$\hat{H}_S = (\hbar\omega_{eg} + \lambda_0) |e\rangle\langle e|, \quad (27)$$

where we have set the energy of the electronic ground state $|g\rangle$ to zero. From the form of \hat{H}_{SB} we identify the system operator $\hat{A}_e = |e\rangle\langle e|$ and the bath operator $\hat{B} = \hat{\Delta}_{eg}(\mathbf{Q})$. We can now define the usual bath correlation function as

$$C(t) = \text{tr}_B \{ \hat{B}(t) \hat{B}(0) \hat{\rho}_B \} = \text{tr}_B \{ \hat{\Delta}(t) \hat{\Delta}(0) \hat{\rho}_B \}, \quad (28)$$

where we have dropped the dependence on bath coordinates in the notation for simplicity. $\hat{\Delta}$ can be thought of as a “gap” operator, that is, as a measure of the energy difference between the ground and excited state at a given nuclear configuration. From now on we will indicate reduced gap correlation functions as

$$\alpha(t) \equiv \text{tr}_B \{ \hat{\Delta}(t) \hat{\Delta}(0) \hat{\rho}_B \}, \quad (29)$$

to distinguish them from the general bath correlation function $C(t)$. Eq. 29 corresponds to the full quantum gap correlation function that one would obtain, e.g., from a quantum simulation on the FMO complex, considering only two electronic levels per molecule and after including the protein environment.

B. Quantum correlation function and energy gap correlation function for harmonic surfaces

In most of the open quantum system approaches used to describe the FMO complex, the bath is taken as an (infinite) set of harmonic oscillators for the environment of each BChl. Each oscillator coordinate is then assumed to be linearly coupled to the electronic excitation of the BChls, i.e. $H_{SB} = |e\rangle\langle e| \otimes \sum_j \kappa_j Q_j$ where κ_j is a coupling constant defined in Tab. II. To establish the connection between the reduced gap operator and this system-bath interaction, we now consider identical shifted harmonic potential surfaces, as sketched in Fig. 3. The quantities defined in the general case in the previous Section III A become,

$$\begin{aligned} \hat{H}_g(\mathbf{Q}, \mathbf{P}) &= \frac{1}{2} \sum_{j=1}^F (P_j^2 + \Omega_j^2 Q_j^2) \\ \hat{H}_e(\mathbf{Q}, \mathbf{P}) &= \hbar\omega_{eg} + \frac{1}{2} \sum_j (P_j^2 + \Omega_j^2 (Q_j - \delta Q_j)^2) \\ &= \hat{H}_g(\mathbf{Q}, \mathbf{P}) + \hat{\Delta}_{eg}(\mathbf{Q}), \end{aligned} \quad (30)$$

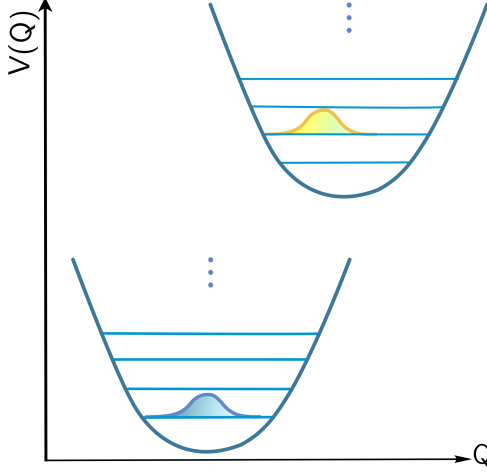


Figure 3. Shifted harmonic identical Born-Oppenheimer surfaces. This model is the one employed in Sec. III B to derive classical and semiclassical expressions for the Fourier transform of the bath correlation function $G(\omega)$ and for the spectral density.

with

$$\hat{\Delta}_{\text{eg}}(\mathbf{Q}) = \hbar\omega_{\text{eg}} + \sum_j \frac{1}{2} \Omega_j^2 \delta Q^2 - \sum_j (\Omega_j^2 \delta Q_j) Q_j, \quad (31)$$

where Ω_j is the frequency of the j -th oscillator. Here, the constant shift λ_0 introduced in Eq. 23 corresponds to the frequently employed reorganization energy $\lambda_0 \equiv \lambda_R = \sum_j \frac{1}{2} \Omega_j^2 \delta Q^2$. Using $Q_j = \sqrt{\hbar/(2\Omega_j)}(a_j^\dagger + a_j)$ and $P_j = i\sqrt{\hbar\Omega_j/2}(a_j^\dagger - a_j)$, Eqs. 30 can also be written as

$$\begin{aligned} \hat{H}_{\text{g}} &= \sum_j \hbar\Omega_j a_j^\dagger a_j \\ \hat{H}_{\text{e}} &= \hat{H}_{\text{g}} + \hbar\omega_{\text{eg}} + \sum_j \hbar\Omega_j X_j - \sum_j \hbar\Omega_j \sqrt{X_j}(a_j^\dagger + a_j). \end{aligned} \quad (32)$$

Here a_j^\dagger and a_j are the bosonic creation and annihilation operators corresponding to the ground state Hamiltonian. We have also introduced the so-called Huang-Rhys factor [54]: $X_j = \frac{\Omega_j}{2\hbar} \delta Q_j^2$. Note that the total Hamiltonian is now in the standard form of an open quantum system model, as in Eq. 1, with the relevant quantities given in Table II.

This model for a few vibrational modes of the chromophores, has been successfully employed to describe the optical properties of molecular aggregates [55–58].

From the expression of the energy gap operator shown in Table II, one obtains the quantum two-time bath correlation function [48]

$$\alpha(t) = 2 \cdot \frac{1}{2\pi} \int_0^\infty J(\omega) \left[\coth\left(\frac{\hbar\omega\beta}{2}\right) \cos(\omega t) - i \sin(\omega t) \right] d\omega \quad (33)$$

where $J(\omega) = 2\pi (\Theta(\omega)j(\omega) - j(-\omega)\Theta(-\omega))$, was defined

in Eq. 17 with

$$j(\omega) = \sum_{j=1}^F \kappa_j^2 \delta(\omega - \Omega_j). \quad (34)$$

In consistency with our definition of the Fourier transform, Eqs. 8 and 18, a factor of 2π has been introduced and appears in Eqs. 33 and 34. Note that $\alpha(t)$ corresponds to the $C(t)$ of Eq. 3.

To establish a connection to the classical correlator, which is real and symmetric, we note that $j(\omega)$ can be obtained from the real part of $\alpha(t)$ via

$$j(\omega) = \frac{1}{\pi} \tanh\left(\frac{\hbar\omega\beta}{2}\right) \int_0^\infty \text{Re}\{\alpha(t)\} \cos(\omega t) dt. \quad (35)$$

This is the expression (up to the constant prefactor $2/\hbar$) used in Refs. [27, 33], to obtain spectral densities. When using this expression to obtain the spectral density from QM/MM simulations one often assumes that $C^{\text{cl}}(t) \approx \text{Re}\{\alpha(t)\}$, following the Standard approximation (see. Appendix A). Then, after a Fourier transform and use of symmetry relations for $G(\omega)$ one finds the following expression,

$$j(\omega) = \frac{1}{2\pi} \tanh\left(\frac{\hbar\omega\beta}{2}\right) G^{\text{cl}}(\omega); \quad \omega > 0. \quad (36)$$

Note that in this section, Eqs 33, 35 and 36, differ by a factor of $1/2$ from those in Ref. [48] due to our definition in Eq. 11.

IV. CLASSICAL AND SEMICLASSICAL LIMITS OF THE CORRELATORS AND SPECTRAL DENSITIES FOR HARMONIC SURFACES

As outlined in the previous section, the harmonic model allows for a simple analytic solution in the quantum mechanical case. Now we will show that the system also has a solution in the classical case. In particular, in this section, we will introduce a model to construct exact relations between the classical gap-correlation and the quantum one. To this end, we will consider classical dynamics in the ground state BO potentials within an initial value representation of the initial state which is consistent with the mixed QM/MM approach. For each initial value, we calculate a trajectory and the corresponding reduced classical energy gap between the two surfaces, i.e. $\Delta(\mathbf{Q}(t), \mathbf{P}(t))$. We then average over many trajectories.

A. Classical equations of motion

The classical equation of motion of the j -th harmonic bath coordinate is $\ddot{Q}_j + \Omega_j^2 Q_j = 0$. Solving this differential equation with the initial condition $(Q_{j0}, P_{j0}) = (Q_j(t=0), P_j(t=0))$ yields the time dependent coordinate trajectories

$$\begin{aligned} Q_j(t) &= Q_j(t; Q_{j0}, P_{j0}) \\ &= Q_{j0} \cos(\Omega_j t) + \frac{P_{j0}}{\Omega_j} \sin(\Omega_j t). \end{aligned} \quad (37)$$

Table II. Expressions of the system bath quantities for the case of two Born-Oppenheimer harmonic surfaces as sketched in Fig. 3.

Quantity	Expression
System Hamiltonian	$\hat{H}_S = (\hbar\omega_{eg} + \lambda_R) e\rangle\langle e $
System-bath Hamiltonian	$\hat{H}_{SB} = e\rangle\langle e \hat{\Delta}(\mathbf{Q})$
Bath Hamiltonian	$\hat{H}_B = \hat{H}_g = \sum_j \hbar\Omega_j a_j^\dagger a_j$
Energy gap operator	$\hat{\Delta}_{eg}(\mathbf{Q}) = \hbar\omega_{eg} + \lambda_R - \sum_j \sqrt{2\hbar\Omega_j^3 X_j} Q_j$
Reduced energy gap operator	$\hat{\Delta}(\mathbf{Q}) = \hat{\Delta}_{eg}(\mathbf{Q}) - (\hbar\omega_{eg} + \lambda_R)$
Reorganization energy	$\lambda_0 = \lambda_R = \sum_j \frac{1}{2} \Omega_j^2 \delta Q_j^2$
Coupling constant	$\kappa_j = \hbar\Omega_j \sqrt{X_j}$
Huang-Rhys factor	$X_j = \Omega_j \delta Q_j^2 / (2\hbar)$
Unitless constant	$\zeta_j = \hbar\Omega_j / (k_B T)$

For each trajectory, the energy gap is then expressed as

$$\begin{aligned} \Delta(t) &= \Delta(t; Q_{j0}, P_{j0}) \\ &= - \sum_j (\Omega_j^2 \delta Q_j) \left(Q_{j0} \cos(\Omega_j t) + \frac{P_{j0}}{\Omega_j} \sin(\Omega_j t) \right) \end{aligned} \quad (38)$$

where the parametric dependence of Q_j and Δ on the initial conditions (Q_{j0}, P_{j0}) has been explicitly indicated.

B. Energy gap correlator

The evaluation of the reduced gap correlation function, Eq. 29, in the classical limit, results in the following expression

$$\begin{aligned} \alpha(t) &= \sum_{jk} \int d\mathbf{P}_0 d\mathbf{Q}_0 \mathcal{W}(\mathbf{Q}_0, \mathbf{P}_0) \times \\ &\quad \Delta(t; Q_{j0}, P_{j0}) \Delta(0; Q_{k0}, P_{j0}) \end{aligned} \quad (39)$$

where $\mathcal{W}(\mathbf{Q}_0, \mathbf{P}_0)$ is the initial distribution and $d\mathbf{P}_0 d\mathbf{Q}_0$ denotes the set of all coordinates, i.e. $d\mathbf{Q}_0 = dQ_{10} \cdots dQ_{M0}$. For harmonic potential surfaces, Eq 19, is time-evolved following Eq. (38). In this Section, we will investigate two different choices for the initial distribution, namely a Boltzmann distribution, as in Ref. 21, and a Wigner distribution which resembles the quantum thermal state. We will refer to the two cases as the classical limit and the semi-classical limit, respectively.

C. Classical and semiclassical correlation functions

1. Classical limit

To obtain the classical limit of the correlator, we choose the Boltzmann distribution for the initial coordinates which corresponds to a purely classical thermal state. The distribution is defined as follows

$$\mathcal{W}^{\text{boltz}}(\mathbf{Q}_0, \mathbf{P}_0) = \prod_j \mathcal{W}_j^{\text{boltz}}(Q_{j0}, P_{j0}), \quad (40)$$

with $\mathcal{W}_j^{\text{boltz}}(Q_{j0}, P_{j0}) = \frac{\beta\Omega_j}{2\pi} e^{-\frac{\beta}{2}(P_{j0}^2 + \Omega_j^2 Q_{j0}^2)}$, and it is normalized to one, i.e., $\int dP_{j0} dQ_{j0} \mathcal{W}_j^{\text{boltz}}(Q_{j0}, P_{j0}) = 1$. Note that $(\Omega_j^2 \delta Q_j)^2 = 2\hbar X_j \Omega_j^3$. Using Eq. 39 and the Boltzmann distribution for initial positions and momenta, we obtain,

$$\alpha_{\text{boltz}}(t) = \sum_j (\hbar\Omega_j)^2 X_j \cos(\Omega_j t) \left(\frac{2}{\zeta_j} \right). \quad (41)$$

Here we have introduced the definition $\zeta_j \equiv \hbar\Omega_j / (k_B T)$. This quantity is also reported in Tab. II.

2. Semiclassical limit

In order to obtain the semiclassical limit, we take the quantum Wigner distribution for the initial coordinates and use it in Eq. 39. The Wigner distribution is given by

$$\mathcal{W}^{\text{wig}}(\mathbf{Q}_0, \mathbf{P}_0) = \prod_j \mathcal{W}_j^{\text{wig}}(Q_{j0}, P_{j0}), \quad (42)$$

where we have used the compact notation

$$\mathcal{W}_j^{\text{wig}}(Q_{j0}, P_{j0}) \equiv 2 \tanh\left(\frac{\zeta_j}{2}\right) e^{-\tanh(\zeta_j/2) \left(\frac{\Omega_j}{\hbar} Q_{j0}^2 + \frac{1}{\hbar\Omega_j} P_{j0}^2 \right)}. \quad (43)$$

The normalization of the Wigner distribution is chosen such that $\int \frac{dP_{j0} dQ_{j0}}{2\pi\hbar} \mathcal{W}_j^{\text{wig}}(Q_{j0}, P_{j0}) = 1$. The resulting expression of the energy gap correlation function is

$$\alpha_{\text{wig}}(t) = \sum_j (\hbar\Omega_j)^2 X_j \cos(\Omega_j t) \coth\left(\frac{\zeta_j}{2}\right). \quad (44)$$

D. Classical and semiclassical spectral densities

The Fourier transform of the correlator $\alpha(t)$, Eq. 8 yields the TDCD $G(\omega)$. After applying it to Eq. 41 and to 44 we obtain

$$G_{\text{boltz}}(\omega) = \pi \sum_j \left(\frac{2k_B T}{\hbar\omega} \right) \kappa_j^2 (\delta(\omega - \Omega_j) + \delta(\omega + \Omega_j)) \quad (45)$$

and for the Wigner distribution

$$G_{\text{wig}}(\omega) = \pi \sum_j \coth\left(\frac{\hbar\omega}{2k_B T}\right) \kappa_j^2 (\delta(\omega - \Omega_j) + \delta(\omega + \Omega_j)). \quad (46)$$

Here $\kappa_j = \hbar\omega\sqrt{X_j}$ as in Tab. II. Now, using Eq. 34 we have

$$G_{\text{boltz}}(\omega) = 2\pi \frac{2k_B T}{\hbar\omega} j(\omega) \quad (47)$$

$$G_{\text{wig}}(\omega) = 2\pi \coth\left(\frac{\hbar\omega}{2k_B T}\right) j(\omega). \quad (48)$$

One can then obtain the corresponding spectral densities $j(\omega)$

$$j(\omega) = \begin{cases} \frac{1}{2\pi} \tanh\left(\frac{\hbar\omega}{2k_B T}\right) \int_{-\infty}^{\infty} e^{i\omega t} \alpha_{\text{wig}}(t) dt \\ \frac{1}{2\pi} \frac{\hbar\omega}{2k_B T} \int_{-\infty}^{\infty} e^{i\omega t} \alpha_{\text{boltz}}(t) dt \end{cases}. \quad (49)$$

We see that the semiclassical Wigner distribution yields the same prefactor as for the Standard approximation described in Section II C while the Boltzmann distribution gives the same prefactor as the Harmonic approximation, also described in Section II C.

V. MODELS FOR SYSTEM-BATH COUPLING - HIGHER ORDER CORRELATORS

As discussed in the introduction, there has been a lot of interest in modeling the exciton dynamics of the FMO complex using open quantum system approaches. These usually require as input a bath two-time correlation function or (equivalently) a spectral density and they rely on the assumption of linear coupling to the bath and on a bath described by harmonic oscillators [59].

In the previous Section III B, we have discussed that this model corresponds to shifted adiabatic BO surfaces of identical curvature. We have shown that in this case, the energy gap two-time correlation function for a classical ground-state propagation is directly proportional to the quantum one and we have extracted the appropriate (frequency dependent) proportionality constant. For other shapes of the potential surfaces involved, one will in general obtain different proportionality constants, although the delta-peaks of the spectral densities can be located at the same energies (the positions are determined by the shape of the ground state potential).

It is not clear, *a priori*, if the approximation of shifted harmonic surfaces (or equivalently linear coupling to a harmonic bath) is a good one for the system under consideration. To gain some insight on this question, from an analysis of QM/MM trajectories, one possibility is to consider higher order correlators. If the approximation of linearly coupled harmonic oscillators is inadequate, one expects that higher order correlators will have a significant relative weight.

We proceed to discuss some properties of correlations of the bath gap operator, Eq. 23. The energy gap operators can be described by a function of the bath coordinates and expanded in terms of these as

$$\hat{\Delta} = \sum_i \xi_i^{(0)} + \sum_i \xi_i^{(1)} Q_i + \sum_{ij} \xi_{ij}^{(2)} Q_i Q_j + \dots \quad (50)$$

When only terms up to first order in Q are significant, as in the case of the Harmonic surfaces in the linear system bath coupling limit, Tab. II, we can write the two-time correlation function as

$$\alpha(t, 0) = \langle \hat{\Delta}(t) \hat{\Delta}(0) \rangle = \sum_{ij} \xi_i^{(1)} \xi_j^{(1)} \langle Q(t) Q_j(0) \rangle. \quad (51)$$

Here, we have excluded the zeroth-order term which corresponds, e.g. to a reorganization energy, and is usually renormalized into the system Hamiltonian. The angular brackets $\langle \dots \rangle = \text{tr}_B \{ \dots, \hat{\rho}_B \}$ indicate thermal averaging over the bath degrees of freedom. Similarly, the three-time correlation function becomes

$$\begin{aligned} \alpha(t', t, 0) &= \langle \hat{\Delta}(t') \hat{\Delta}(t) \hat{\Delta}(0) \rangle \\ &= \sum_{ijk} \xi_i^{(1)} \xi_j^{(1)} \xi_k^{(1)} \langle Q_i(t') Q_j(t) Q_k(0) \rangle. \end{aligned} \quad (52)$$

In the case of a harmonic bath, the three-time correlation function will vanish, and in general any odd permutation of the harmonic bath coordinates will vanish.

However, if one considers the case where one retains the second order term in Eq. 50, the two-time correlator will become:

$$\alpha(t, 0) = \sum_{ijkl=0} \Xi_{ij} \Xi_{kl} \langle Q_{ij}(t) Q_{kl}(0) \rangle, \quad (53)$$

where we have defined Ξ_{ij} and $Q_{ij}(t)$ as

$$\Xi_{ij} = \begin{cases} 0 & ; i = j = 0 \\ \xi_i^{(1)} & ; j = 0 \wedge i \neq 0 \\ \xi_j^{(1)} & ; i = 0 \wedge j \neq 0 \\ \xi_{ij}^{(2)} & ; i, j \neq 0 \end{cases}$$

$$Q_{ij}(t) = \begin{cases} 0 & ; i = j = 0 \\ Q_i(t) & ; j = 0 \wedge i \neq 0 \\ Q_j(t) & ; i = 0 \wedge j \neq 0 \\ Q_i(t) \cdot Q_j(t) & ; i, j \neq 0 \end{cases}.$$

Analogously the three-time correlator becomes

$$\alpha(t', t, 0) = \sum_{ijklmn=0} \Xi_{ij} \Xi_{kl} \Xi_{mn} \langle Q_{ij}(t') Q_{kl}(t) Q_{mn}(0) \rangle. \quad (54)$$

If the bath is harmonic, it is straightforward to show that all terms with an odd number of coordinate operators in the averages will vanish. Yet, we see that in general, unless the coupling to the bath coordinates is linear and the bath consists of Harmonic oscillators, the three-point correlator will not vanish. It may therefore be necessary to go beyond the simple description using only the two-time correlator.

VI. APPLICATION TO THE FMO COMPLEX

In this section, we apply the approximations discussed in Section II C, to the energy gap trajectories obtained from the

mixed QM/MM simulations for the FMO complex of *Prosthecochloris aestuarii* as carried out recently by us in Ref. [27]. The nuclear trajectories were obtained by classical MD using the AMBER 99 force field. An isothermal-isobaric (NPT) ensemble was employed in the MD simulations. For the calculation of the energy gap, snapshots of the nuclear coordinates were taken at every 4 fs. For each ground state configuration, the gap was obtained by computing the energy corresponding to the Q_y transition of the BChl's using time-dependent time-dependent density functional theory with BLYP functional within the Tamm-Dancoff approximation. More details on the computation can be found in Ref. [27].

A. TDCD and spectral density from mixed QM/MM with a posteriori semiclassical corrections

Using the energy gap trajectories obtained in Ref. [27], we evaluated the different semiclassical approximations as reported in Tab. I. We denote the time-points at which the energy gap is calculated by t_i and the corresponding energy gap by X_i where $i = 0 \dots N-1$ runs over the N the time-points. As in Ref. [27] we evaluated the correlator by using a discrete representation, which implements the k -th element of the two-time correlator as

$$C_k = \frac{1}{(N-k)m^{(2)}} \sum_{i=1}^{N-k} (X_i - \bar{X}) (X_{i+k} - \bar{X}) \quad (55)$$

where $m^{(2)} = \sum_i^N (X_i - \bar{X})^2 / N$ is the variance and \bar{X} is the mean. Here, one assumes that the $N-k$ values X_i give a faithful initial distribution which reproduces the Boltzmann distribution. To minimize spurious effects in the Fourier transform, we multiplied the time trace by a Gaussian of variance $\sigma_{\text{gaussian}}^2 = 0.09 \cdot t_{\text{max}}^2 = 2.304 \cdot 10^5 \text{ fs}^2$ with $t_{\text{max}} = 1600 \text{ fs}$, the length of the correlation function (as reported in [27]). The Gaussian is normalized to have unitary area in frequency domain [60] following our definition of the Fourier transform in Eq. 8. Next, we computed the different semiclassical quantities of Table I using our initial time trace.

In Figure 4, we show the temperature-dependent coupling densities TDCDs (as defined in Eq. 8), for site 1 of the FMO complex (site 1 at 77K and 300K) evaluated using the different approximations listed in Table I column two. We notice how, as expected, there are little differences between the approximations at low frequencies. Only at higher frequencies the TDCD differs significantly for each approach. The Egelstaff approximation incorrectly predicts a negative spectral density for low frequencies in this case and was therefore not shown in the plots.

Similarly, in Fig. 5, we show the asymmetric component of the TDCD ($J(\omega) = G_{\text{asym}}(\omega)$) for site 1 of the FMO complex at 77K and 300K evaluated with the different approximation methods. The trend is similar to what we saw for the TDCD. From the general definition of each semiclassical correction, it isn't clear which one is most accurate. To better reason on which one to choose we evaluated the three point correlator (Sec.VI C) to see if the approximation of a Harmonic bath is

valid. The motivation for this procedure was given in Section V.

B. Analysis of prefactors in terms of temperature dependence of the spectral density

From our discussion in Section I, we recall that many open quantum system approaches rely on the assumption of linear coupling to a bath of harmonic oscillators. This leads to a temperature-independent spectral density. Inspection of Fig 5 shows that the asymmetric TDCD (which is directly proportional to the spectral density) obtained from the QM/MM is not similar at different temperatures. This is more apparent at higher frequencies. The source of this temperature dependence could be due to the fact that the MD bath is not fully harmonic or that the coupling is not completely linear (it might also be possible that the MD is not fully converged). The reason for this temperature dependence is still not immediately clear to us, and we leave this for further studies. We would need to run longer QM/MM trajectories to improve the statistics and further check convergence of the distributions. Nevertheless, based on the most common assumption in the open quantum system approaches, we suggest that the relative temperature-independence is a criterium to select the best approximation for the spectral density. In Fig. 6, we compare the asymmetric TDCD ($J(\omega) = 2\pi j(\omega)$; $\omega > 0$) obtained using the Standard and the Harmonic approximations. It is clear by comparing panel a) and b), that only the Harmonic correction leads to a temperature-independent spectral density. In the bottom panels, c) and d) we compare the asymmetric TDCD averaged over the seven sites, with the experimental asymmetric TDCD. The asymmetric TDCD is obtained from the spectral density as defined in Eq. 17. Further, since in Refs [29, 30, 48], Eq. 11 is defined without the factor 1/2, the experimental spectral density is rescaled by 1/2 for comparison. From panel e) and f) of Fig. 6, we see that the Harmonic curve is in good agreement with experiment. Results for all sites at both temperatures are reported in the Supplementary information, Appendix B. The standard asymmetric component $J(\omega) = G_{\text{asym}}(\omega)$ shown in Fig. 6 panel a), corresponds to the spectral density in Ref. [27] if one multiplies the Shim [61] result by $2\pi \cdot \tanh(\omega\beta\hbar/2)/\tanh(\nu\beta\hbar/2)$ to obtain $J(\omega)$ (here $\nu = \omega/(2\pi)$). The analysis of the temperature dependence of the prefactors for the spectral density suggests that the Harmonic approximation is the correct choice for the FMO complex rather than the Standard one, even though in the later case the agreement with the experimental FLN narrowing results is better. This analysis, is bolstered by the evidence provided by the model in Section III B, and the higher order correlator results, which will be presented in the next Section.

C. Higher-order correlation function

From the theory of discrete processes, similarly to Eq. 55, we see that the (k, j) -th element of the three-time correlator

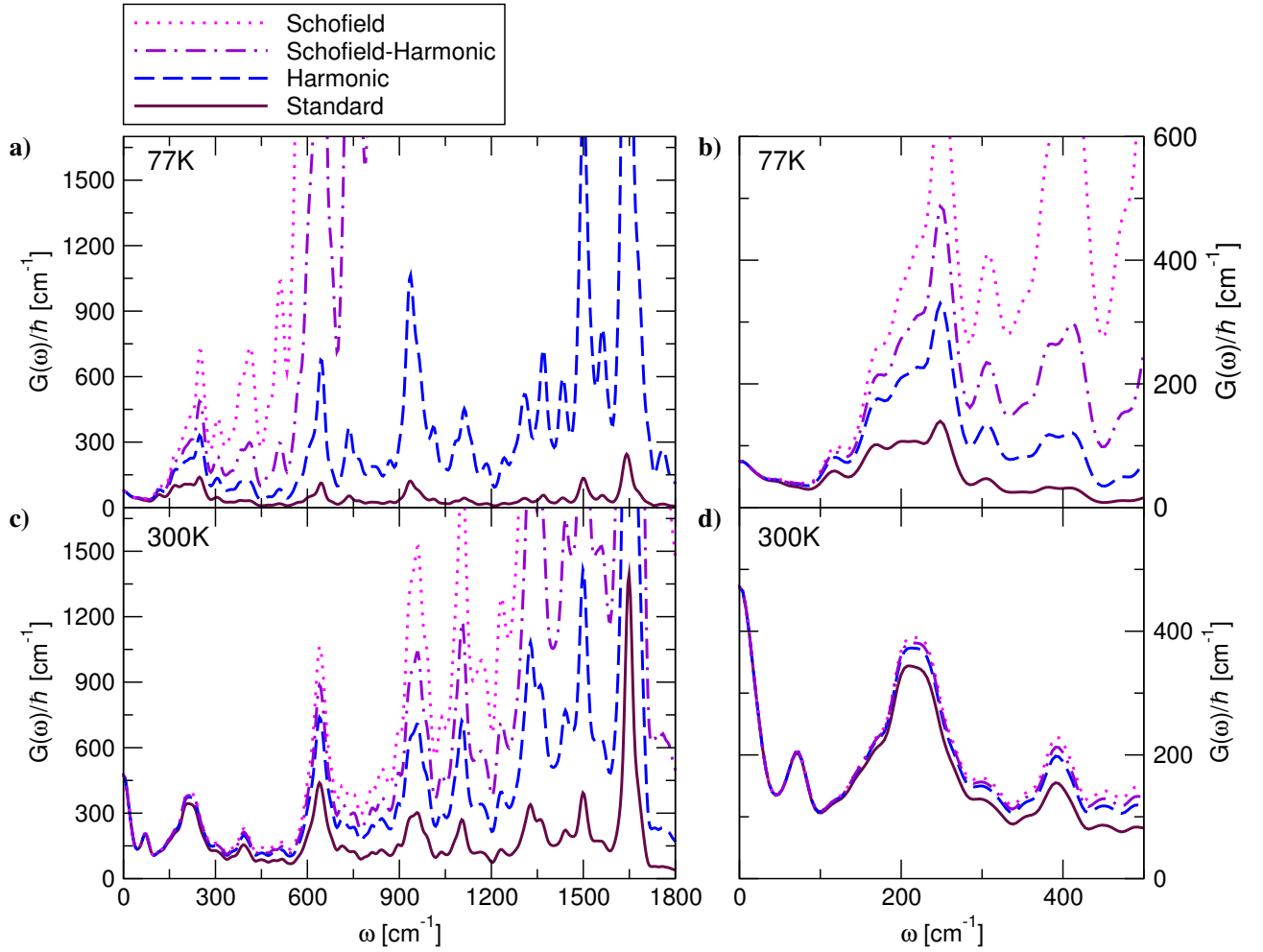


Figure 4. Temperature-dependent coupling densities $G(\omega)$ obtained with each of the Standard, Harmonic, Schofield and Schofield-Harmonic corrections as listed in Tab. I, column two. In particular in panel a) results are at 77K and in panel c) 300K. Panels b) and d) display the low frequency region of figures a) and c) respectively. These results are obtained after multiplication of the time series with a Gaussian window function as described in the Section VIA.

is

$$C(k, j) = \frac{1}{(N - k - j)m^{(3)}} \times \sum_{i=1}^{N-k-j} (X_i - \bar{X}) (X_{i+k} - \bar{X}) (X_{i+k+j} - \bar{X}) \quad (56)$$

where $m^{(3)} = \sum_i^N (X_i - \bar{X})^3 / N$ is the third moment and \bar{X} is the mean. We compare the two correlators by dividing them by increasing powers of the standard deviation $\sqrt{m^{(2)}}$. The results for site 1 of the FMO complex at 77 and 300K are reported in Fig. 7. For the two-time correlator, Fig. 7 panels a) and b), we see correlations up to at least 1000 time steps, while for the three-time correlator, panels c), d), e) and f), we see a rather flat profile with values about two orders of magnitude smaller than the largest value of the two-time correlations. This is observed for all sites and temperatures (Results for all sites can be found in the Supplementary information, Appendix B).

This means that since we find a small and roughly flat three-time correlator, the linear coupling to a harmonic bath assumption is probably good. In fact, as described in Sec. V this case corresponds to linear coupling to the bath and Gaussian correlated bath operators. Of course, there may be other fortuitous cases in which the three-time correlator is roughly zero and the bath is not harmonic. Further, this comparison is based on the order of magnitude of the correlations, the three-time correlator is only much smaller. It may be that for some modes of the system, certain frequencies, present in the three-time correlator's two dimensional Fourier transform give a more important contribution to the dynamics than other frequencies present in the spectral density. Nonetheless, the above result encourages the idea that the assumption of linear coupling and harmonic bath is valid. This, in turn, implies that one should use the Harmonic semiclassical correction in Sec. IIC, which is also consistent with the prefactor found in III.

One a final note, to confirm with certainty that the bath is Harmonic, one should evaluate higher order correlators, be-

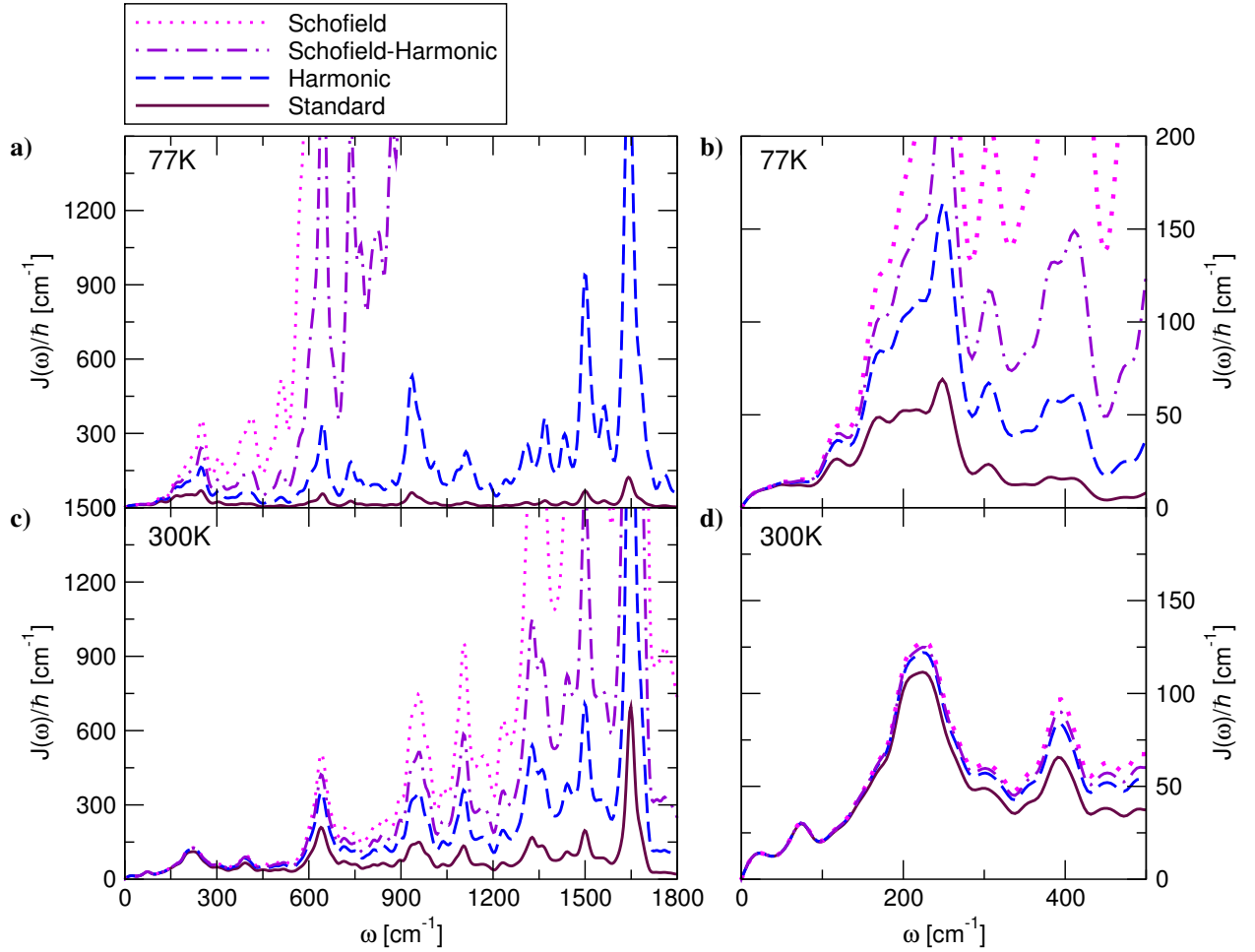


Figure 5. Asymmetric component of temperature-dependent coupling density $J(\omega) \equiv G_{\text{asym}}(\omega)$; obtained with each of the Standard, Harmonic, Schofield and Schofield-Harmonic corrections as listed in Tab. I, column three. In particular in panel a) results are at 77K and in panel c) 300K. Panels b) and d) display the low frequency region of figures a) and c) respectively. These results are obtained after multiplication of the time series with a Gaussian window function as described in the Section VI A. Note that the spectral density, as defined in Eq. 17 can be obtained by dividing $J(\omega)$ by 2π .

yond the three-time correlator. However, to obtain a statistically relevant estimate, much longer time dependent energy gap trajectories, which are expensive in terms of the QM/MM propagation, would be required. Work in this direction is being carried out in our groups.

VII. CONCLUSIONS

In this work, we have investigated the connection between the gap correlation function extracted from ground state QM/MM and the bath spectral density used as input in many open quantum system approaches.

One important point is that the classical bath correlation function is real while the quantum mechanical one is generally complex. There exist several semiclassical *a posteriori* corrections which aim to fix this and we have employed them on our time traces to recover a part of the imaginary component.

The discussed prefactors originate from general expansions in orders of \hbar and do not include information on the specific type of system-bath coupling, etc. We have investigated two simple models and found that the prefactors obtained correspond to two of the general semiclassical expressions. Thus, we have linked the semiclassical limits with a microscopic potential energy surface picture.

We have shown that the gap-correlation function extracted from ground state QM/MM only corresponds to the fully quantum excited state calculations in the case of shifted parabolas. This model for a few vibrational modes of the chromophores has been successfully used to describe the optical properties of molecular aggregates. Including only a finite number of internal vibrations is probably a good approximation for molecules in the gas phase or suprafluid Helium nanodroplets [58]. However, for molecules in solution or when a protein environment is present it is no longer a good approximation to include only a few (undamped) modes. In particular, one has to take into account the interaction of

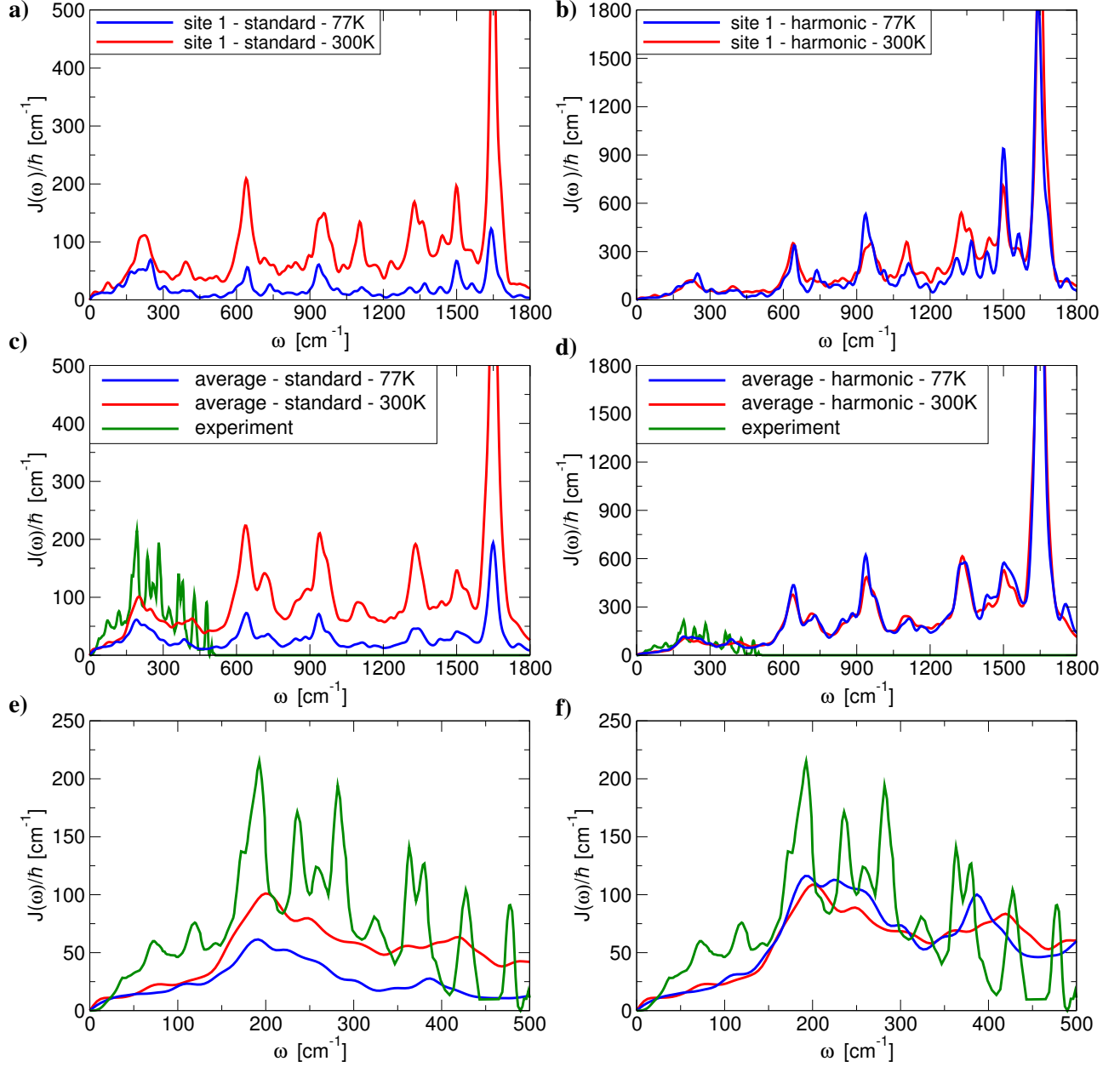


Figure 6. Panel a) comparison of the asymmetric component of temperature-dependent coupling density $J(\omega) \equiv G_{\text{asym}}(\omega)$; for site 1 for the Fenna-Matthews-Olson complex, obtained with the Standard approximation (Table I first line third column) at 77K and at 300K. Panel b) comparison of $J(\omega)$ obtained for site 1 with the Harmonic approximation (Table I second line third column) at 77K and at 300K. We see clearly that the Harmonic prefactor gives a roughly temperature independent $J(\omega)$, while large differences are seen using the Standard prefactor. This consideration can also be made for plots in panels c) and d) where one sees $J(\omega)$ averaged over all sites. In particular, Panel c) shows $J(\omega)$ averaged over all seven sites calculated with the Standard approximation at 77 and 300K and the green curve corresponds to the experimental spectral density rescaled by π (a factor 2π comes from Eq. 14 and a factor $1/2$ comes from Eq. 11) to obtain $J(\omega)$ as defined in Eq. 17 [29, 30]. Panel d) shows $J(\omega)$ averaged over all seven sites calculated with the Harmonic approximation at 77 and 300K and again the green curve corresponds to the experimental spectral density [29, 30]. The agreement with the experimental (green) spectral density is better with the Harmonic approximation than with the Standard approximation. Panels e) and f) correspond to the same quantities as those of panels c) and d) in the low frequency region, here we note that both approximations are roughly equivalent for $\frac{\hbar\omega}{k_B T} < 1$ (e.g at $T = 77$ K for $\omega < 55$ cm⁻¹ and at $T = 300$ K for $\omega < 200$ cm⁻¹). Note that the spectral density, as defined in Eq. 17 can be obtained by dividing $J(\omega)$ by 2π .

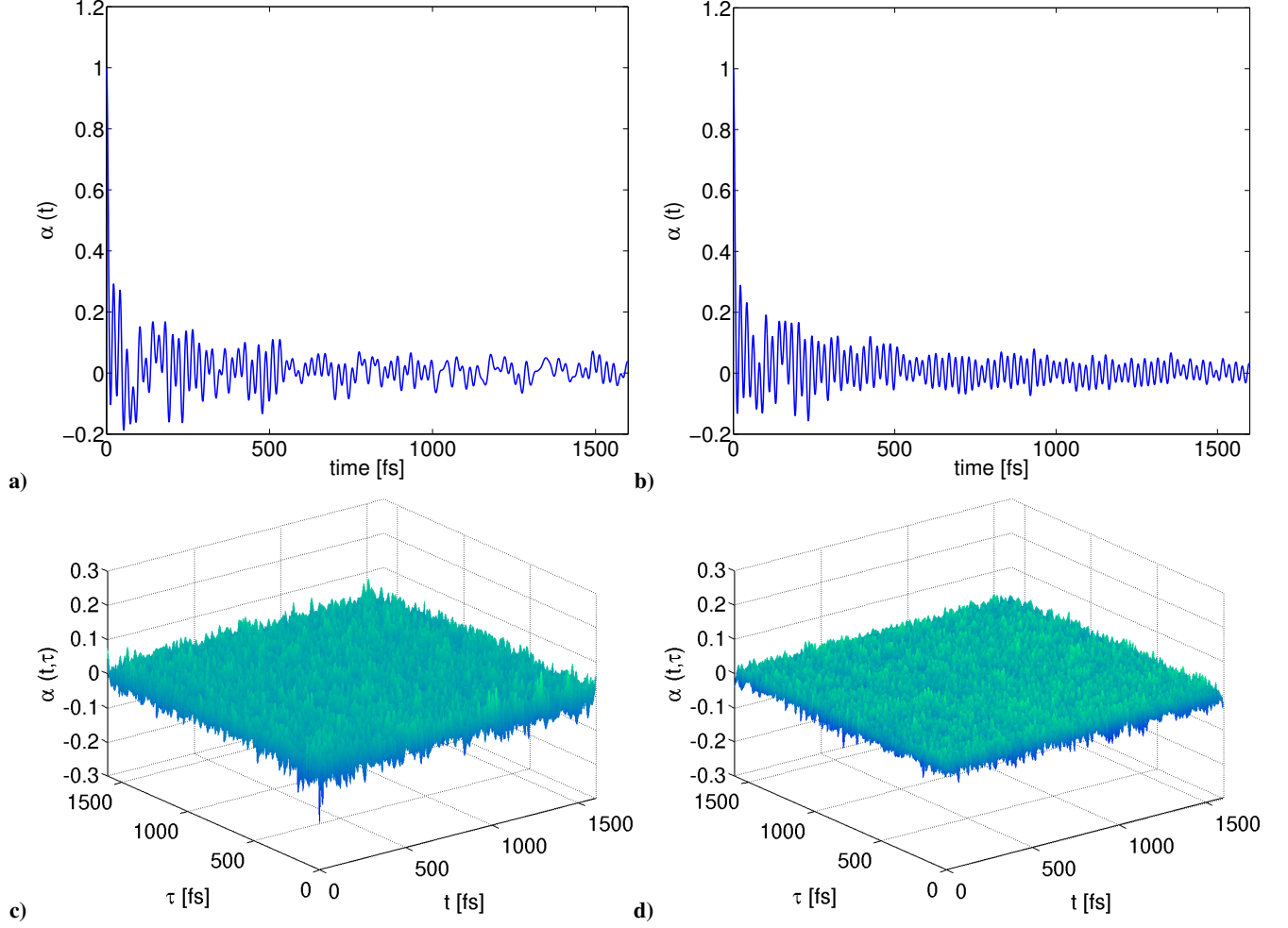


Figure 7. Panel a): Two-time correlation function of the energy gap fluctuations of site 1 of the FMO complex, normalized by $m^{(2)}$ at 77K as in Eq. 55. Panel b): Two-time correlation function for site 1 at 300K. Panel c) Three-time correlation function of the energy gap fluctuations of site 1 of the FMO complex, as defined in Eq. 56 multiplied by $m^{(3)} / (\sqrt{m^{(2)}})^3$ at 77K. Panel d) Three-time correlation function for site 1 at 300K.

the vibrations with the environment in addition to the direct interaction of the electronic excitation with the environment. For this general situation, it is no longer clear if the model of shifted harmonic potential surfaces is indeed a good description of the system.

Therefore, we have investigated whether the approximation of harmonic bath and linear coupling is accurate for our QM/MM calculations for the FMO photosynthetic complex by computing the next higher order correlator beyond the two-time correlator. The three-point correlator seems to give a small contribution which, while not being conclusive, suggests to us that the Harmonic/linear coupling model is a good approximation. The analysis of the temperature dependence of prefactors for the spectral density also suggests that the Harmonic approximation is preferred to use for the FMO complex, and perhaps other photosynthetic complexes, rather than the Standard one. Having made these choices, the theoretical results are in reasonably good agreement with the experimental spectral density. These result in a much better agreement than in our previous work, which underestimated the magnitude of the spectral density [27] and than other QM/MM calculations [26] which overestimate the coupling to the bath by one order of magnitude.

Finally, we have explained the link between bath correlation function and gap correlation function and found models under which the gap correlation function can actually be viewed as a general open quantum system bath correlation function.

ACKNOWLEDGMENTS

We thank Dr. Semion Saikin, for his useful advice and Gerhard Ritschel for going over the manuscript. A. E. acknowledges financial support from the DFG under Contract No. Ei 872/1-1. S. V. and A. A. G. acknowledge support from the Center for Excitons, an Energy Frontier Research Center funded by the U.S. Department of Energy, Office of Science and Office of Basic Energy Sciences under Award Number DE-SC0001088 as well as support from the Defense Advanced Research Projects Agency under award number N66001-10-1-4060. S. V. and A. A.-G. acknowledge support from the Harvard Quantum Optics center.

Appendix A: Semiclassical approximations to the quantum TDCD

The first and most simple approximation is known as the standard approximation [42, 44, 62], and consists in assuming that $C(t) \simeq C^{\text{cl}}(t)$, i.e one assumes that the quantum correlation function is roughly equal to the zeroth order term in its \hbar expansion. Then, taking the Fourier transform and using the appropriate Eq. 12 one finds,

$$G^{\text{std}}(\omega) = \frac{2}{1 + e^{-\beta\hbar\omega}} G^{\text{cl}}(\omega). \quad (\text{A1})$$

We see that this becomes a good approximation for small \hbar or also, for small ω .

The next approximation is known as the “harmonic” approximation [40–42], which corresponds to taking the first order term in the expansion of Eq.7 with respect to \hbar , and then using $C(t) \simeq C^{\text{cl}}(t)$. After Fourier Transformation and substitution using Eq. 14, one arrives to the final expression Note that this approximation doesn’t assume a harmonic bath, but turns out to be exact in the case of a system coupled to a bath of harmonic oscillators as shown in Ref. [35].

The third approximation is due to Schofield [51] and comes from a combination of the standard and harmonic approximations, expanding to first order separately the imaginary and real parts of $C(t)$ and Fourier transforming to obtain

$$G^{\text{scho}}(\omega) = e^{\beta\hbar\omega/2} G^{\text{cl}}(\omega). \quad (\text{A2})$$

The fourth approximation is the Egelstaff approximation [52] which originates from assuming that $C(t) = C^{\text{cl}}\left(\sqrt{t(t + i\beta\hbar)}\right)$ and taking the Fourier transform to arrive at the final expression

$$G^{\text{egel}}(\omega) = e^{\beta\hbar\omega/2} \int_{-\infty}^{\infty} e^{i\omega t} C^{\text{cl}}\left(\sqrt{t^2 + (\beta\hbar/2)^2}\right) dt. \quad (\text{A3})$$

The same ansatz on $C(t)$ can be used to obtain the Schofield approximation, by expanding to first order and subsequently Fourier transforming.

Finally, the last approximation we wish to recall can be obtained by taking the logarithmic average of the Schofield and Harmonic approximations thus obtaining

$$G^{\text{s-h}}(\omega) = e^{\beta\hbar\omega/4} \sqrt{\frac{\beta\hbar\omega}{1 - e^{-\beta\hbar\omega}}} G^{\text{cl}}(\omega). \quad (\text{A4})$$

From these derivations, it is clear that in general it is difficult to identify the best approximation. The Egelstaff approximation doesn’t always satisfy the fact that $G(\omega) \geq 0$ while the other approximations do. Then, all apart from the Egelstaff have the constraint that $G(0) = G^{\text{cl}}(0)$. As described in Ref. [40], one can also check that the Harmonic approximation is exact in the case of linear coupling to a bath of harmonic oscillators while the Egelstaff approximation is the most accurate for exponential coupling to harmonic coordinates. For the other expressions it is unclear which will be best for a generic bath.

Appendix B: Supplementary information

1. Two and three-time correlation functions for all site of the fmo complex

In this Section we report the two and three-time correlation functions for the energy gap fluctuations of the FMO complex as discussed in the text for all seven sites of the complex and for both temperatures, 77 and 300K. The functions are rescaled by increasing powers of the standard deviation

$\sqrt{m^{(2)}}$ as a means of comparison. We notice, by comparing panels a) and b) to c) and d) in Figures 8-14, that the three-time correlation function is always much smaller in amplitude than the corresponding two-time autocorrelation function. This supports the idea that the harmonic bath and linear coupling approximations are good for this system.

2. Harmonic spectral densities for all site of the fmo complex

Here, we report $J(\omega)$ the asymmetric component of $G(\omega)$ as described in the text for all temperatures and sites of the

FMO complex. In Figures 15 and 16, we see that the Harmonic approximation gives a roughly temperature independent quantity for all sites. Further, on this scale the spectral densities do not differ largely between the different sites.

-
- [1] S. Jang, M. D. Newton, and R. J. Silbey, *J. Phys. Chem. B* **111**, 6807 (2007)
 - [2] M. Mohseni, P. Rebentrost, S. Lloyd, and A. Aspuru-Guzik, *J. Chem. Phys.* **129**, 174106 (2008)
 - [3] M. B. Plenio and S. F. Huelga, *New J. Phys.* **10**, 113019 (2008)
 - [4] P. Rebentrost, M. Mohseni, I. Kassal, S. Lloyd, and A. Aspuru-Guzik, *New J. Phys.* **11**, 033003 (2009)
 - [5] J. Cao and R. J. Silbey, *J. Phys. Chem. A* **113**, 13825 (2009)
 - [6] A. Ishizaki and G. R. Fleming, *Proc. Natl. Acad. Sci.* **106**, 17255 (2009)
 - [7] A. Ishizaki and G. R. Fleming, *The Journal of Physical Chemistry B* **115**, 6227 (2011)
 - [8] M. Sarovar, G. R. Fleming, and K. B. Wahley, *Nat. Phys.* **6**, 462 (2010)
 - [9] D. Abramavicius and S. Mukamel, *J. Chem. Phys.* **133**, 064510 (2010)
 - [10] J. Wu, F. Liu, Y. Shen, J. Cao, and R. J. Silbey, *New J. Phys.* **12**, 105012 (2010)
 - [11] J. Moix, J. Wu, P. Huo, D. Coker, and J. Cao, *J. Phys. Chem. Lett.* **2**, 3045 (2011)
 - [12] C. Kreisbeck, T. Kramer, M. Rodriguez, and B. Hein, *J. Chem. Theory and Comput.* **7**, 2166 (2011)
 - [13] N. Skochdopole and D. A. Mazziotti, *J. Phys. Chem. Lett.* **2**, 2989 (2011)
 - [14] G. Ritschel, J. Roden, W. T. Strunz, A. Aspuru-Guzik, and A. Eisfeld, *J. Phys. Chem. Lett.* **2**, 2912 (2011)
 - [15] P. Rebentrost and A. Aspuru-Guzik, *J. Chem. Phys.* **134**, 101103 (2011)
 - [16] N. Singh and P. Brumer, *Faraday Discuss.* **153**, 41 (2011)
 - [17] N. Singh and P. Brumer, arXiv:1106.5911v1(2011)
 - [18] L. A. Pachón and P. Brumer, *Phys. Chem. Chem. Phys.* **14**, 10094 (2012)
 - [19] S. Vlamings and R. J. Silbey, arXiv:1111.3627v1(2011)
 - [20] F. Caruso, S. K. Saikin, E. Solano, S. Huelga, A. Aspuru-Guzik, and M. B. Plenio, *Phys. Rev. B* **85**, 125424 (2012)
 - [21] M. Mohseni, A. Shabani, S. Lloyd, and H. Rabitz, arXiv:1104.4812v1(2011)
 - [22] J. Zhu, S. Kais, P. Rebentrost, and A. Aspuru-Guzik, *J. Phys. Chem. B* **115**, 1531 (2011)
 - [23] J. Roden, A. Eisfeld, W. Wolff, and W. T. Strunz, *Phys. Rev. Lett.* **103**, 058301 (2009)
 - [24] I. de Vega, *Journal of Physics B: Atomic, Molecular and Optical Physics* **44**, 245501 (2011)
 - [25] J. Milton, "Areopagitica: A speech for the liberty of unlicensed printing to the parliament of england," (1644)
 - [26] C. Olbrich, T. L. C. Jansen, J. Liebers, M. Aghtar, J. Strümpfer, K. Schulten, J. Knoester, and U. Kleinekathöfer, *J. Phys. Chem. B* **115**, 8609 (2011)
 - [27] S. Shim, P. Rebentrost, S. Valleau, and A. Aspuru-Guzik, *Biophys. J.* **102**, 649 (2012)
 - [28] C. Olbrich, J. Strümpfer, K. Schulten, and U. Kleinekathöfer, *J. Phys. Chem. Lett.* **2**, 1771 (2011)
 - [29] M. Wendling, T. Pullerits, M. A. Przyjalowski, S. I. E. Vulto, T. J. Aartsma, R. van Grondelle, and H. van Amerongen, *J. Phys. Chem. B* **104**, 5825 (2000)
 - [30] J. Adolphs and T. Renger, *Biophys. J.* **91**, 2778 (2006)
 - [31] I. P. Mercer, I. R. Gould, and D. R. Klug, *J. Phys. Chem. B* **103**, 7720 (1999)
 - [32] C. Olbrich and U. Kleinekathöfer, *J. Phys. Chem. B* **114**, 12427 (2010)
 - [33] A. Damjanović, I. Kosztin, U. Kleinekathöfer, and K. Schulten, *Phys. Rev. E* **65** (2002)
 - [34] S. A. Egorov and B. J. Berne, *J. Chem. Phys.* **107**, 6050 (1997)
 - [35] S. A. Egorov, K. F. Everitt, and J. L. Skinner, *J. Phys. Chem. A* **103**, 9494 (1999)
 - [36] S. A. Egorov, E. Rabani, and B. J. Berne, *J. Phys. Chem. B* **103**, 10978 (1999)
 - [37] H. Kim and P. J. Rossky, *J. Phys. Chem. B* **106**, 8240 (2002)
 - [38] R. Ramírez, T. López-Ciudad, P. Kumar P, and D. Marx, *J. Chem. Phys.* **121**, 3973 (2004)
 - [39] J. L. Skinner and K. Park, *J. Phys. Chem. B* **105**, 6716 (2001)
 - [40] L. Frommhold, *Cambridge Monographs on Atomic, Molecular, and Chemical Physics*, 1st ed., Vol. 2 (Cambridge University Press, 1993)
 - [41] P. H. Berens, G. M. White, and K. R. Wilson, *J. Chem. Phys.* **75**, 515 (1981)
 - [42] B. J. Berne and G. D. Harp, "On the calculation of time correlation functions," in *Advances in Chemical Physics* (John Wiley and Sons, Inc., 1970) pp. 63–227, ISBN 9780470143636
 - [43] D. W. Oxtoby, "Vibrational population relaxation in liquids," in *Advances in Chemical Physics* (John Wiley and Sons, Inc., 1981) pp. 487–519
 - [44] S.-C. An, C. J. Montrose, and T. A. Litovitz, *J. Chem. Phys.* **64**, 3717 (1976)
 - [45] H.-P. Breuer and F. Petruccione, *The Theory of Open Quantum Systems* (Oxford University Press, New York, 2002)
 - [46] Y. Yan and R. Xu, *Ann. Rev. Phys. Chem.* **56**, 187 (2005)
 - [47] F. Barocchi, M. Moraldi, and M. Zoppi, *Phys. Rev. A* **26**, 2168 (1982)
 - [48] V. May and O. Kühn, *Charge and Energy Transfer Dynamics in Molecular Systems* (Wiley-VCH Verlag, Weinheim, 2004)
 - [49] This means that when comparing to these definitions we need

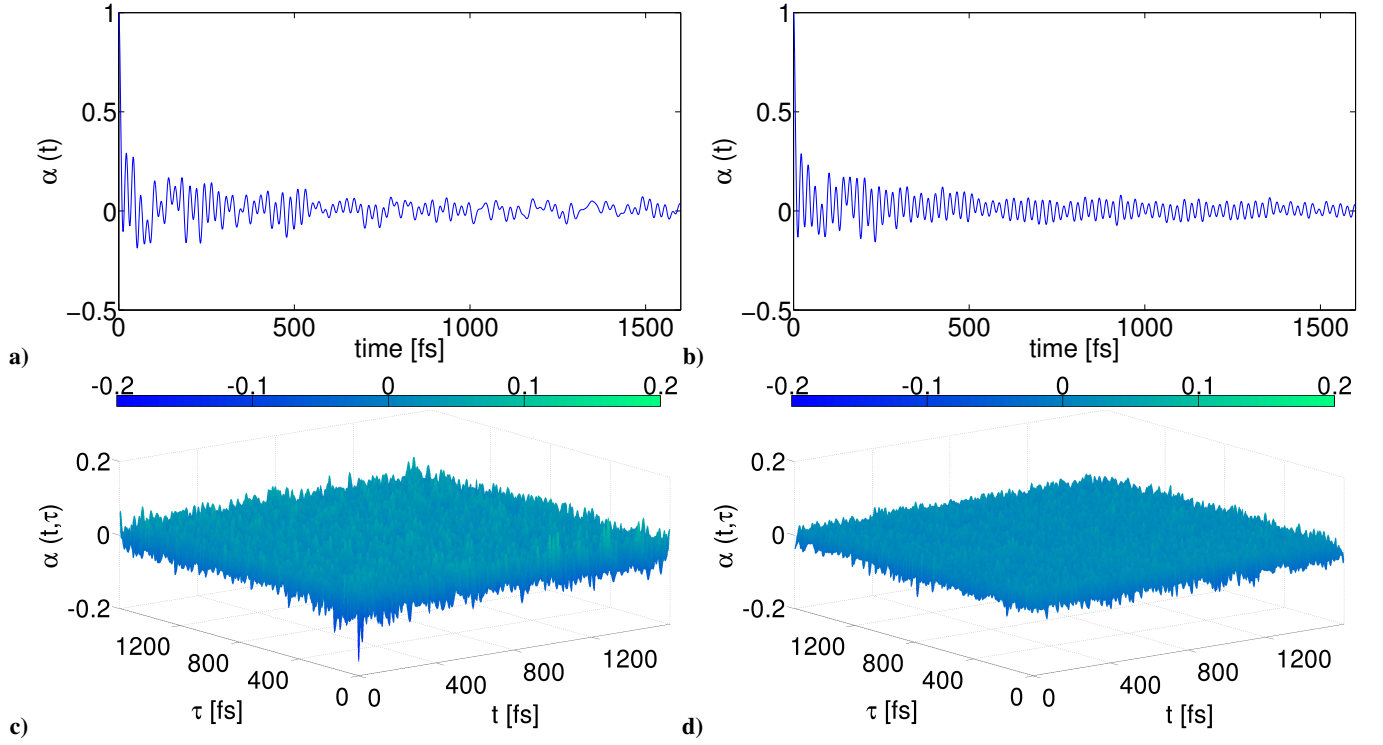


Figure 8. Panel a): Two-time correlation function of the energy gap fluctuations of site 1 of the FMO complex, normalized by $m^{(2)}$ at 77K as discussed in the text. Panel b): Two-time correlation function for site 1 at 300K. Panel c) Three-time correlation function of the energy gap fluctuations of site 1 of the FMO complex, as discussed in the text and multiplied by $m^{(3)} / \left(\sqrt{m^{(2)}} \right)^3$ at 77K. Panel d) Three-time correlation function for site 1 at 300K.

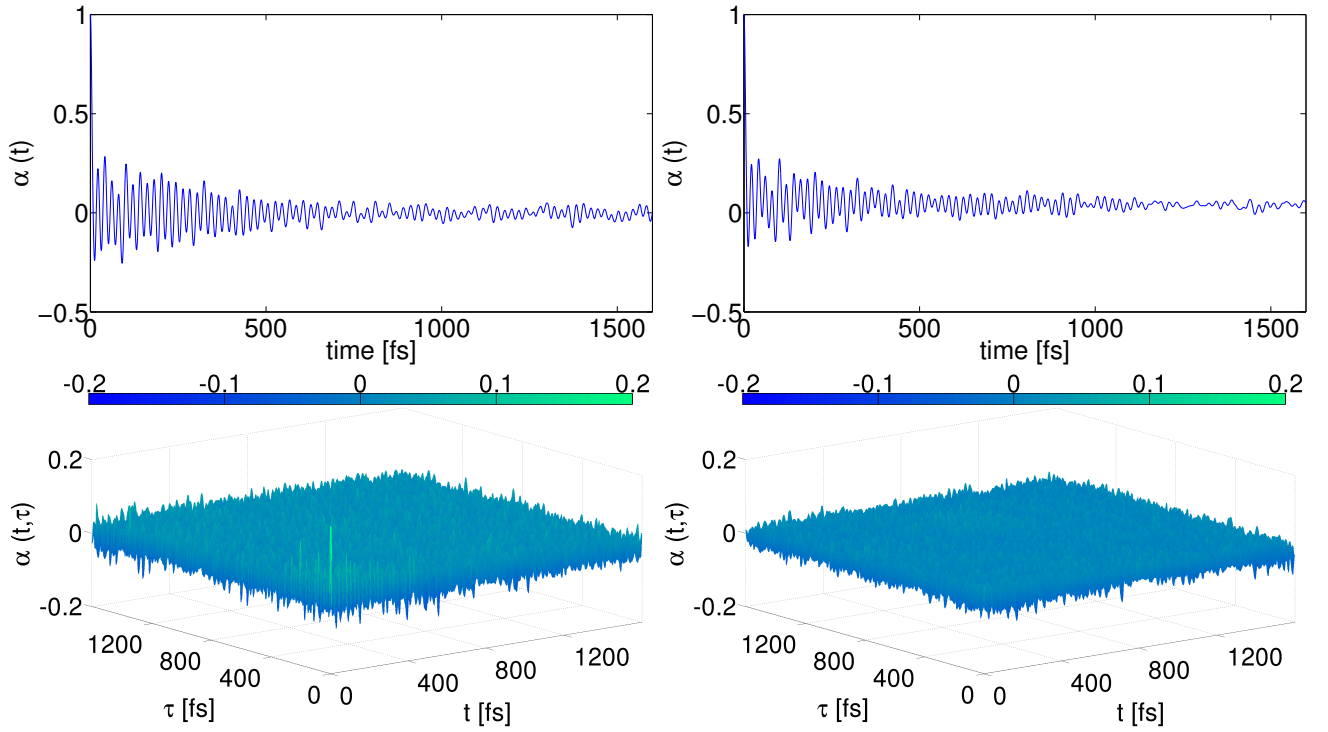


Figure 9. Same as for Fig. 8 but for site 2 of the FMO complex.

to multiply $G_{\text{asym}}(\omega)$ by two.

- [50] Let us remark that using the symmetric $G_{\text{sym}}(\omega)$ one has $j(\omega) = G_{\text{sym}}(\omega)/(2\pi)$; $\omega \geq 0$ and $G_{\text{sym}}(\omega) = 2\pi \cdot j(\omega)$; $\omega \geq 0$ $G_{\text{sym}}(\omega) = 2\pi \cdot j(-\omega)$; $\omega < 0$;
- [51] P. Schofield, *Phys. Rev. Lett.* **4**, 239 (1960)
- [52] P. Egelstaff, *Advances in Physics* **11**, 203 (1962)
- [53] Approximations such as the transition density cube [63] can be employed to obtain couplings between the local excited states. More sophisticated models that include polarization effects [64, 65] can also be employed for this purpose.
- [54] E. S. Medvedev and V. I. Osherov, *Radiationless Transitions in Polyatomic Molecules*, Springer Series in Chemical Physics, Vol. 57 (Springer-Verlag, 1995)
- [55] F. C. Spano, *J. Am. Chem. Soc.* **131**, 4267 (2009)
- [56] P. O. J. Scherer and S. F. Fischer, *Chem. Phys.* **86**, 269 (1984)
- [57] J. Guthmuller, F. Zutterman, and B. Champagne, *The Journal of Chemical Physics* **131**, 154302 (2009)
- [58] J. Roden, A. Eisfeld, M. Dvořák, O. Bünermann, and F. Stienkemeier, *J. Chem. Phys.* **134**, 054907 (2011)
- [59] Note that there are two common approximations for which the information on the system bath coupling is entirely described by the two-time bath correlation function, namely linear response theory and second order perturbation theory in system bath coupling.
- [60] The variance in frequency domain is $\sigma_{\omega}^2 = 4.3403 \cdot 10^{-6} \frac{1}{\text{fs}^2}$.
- [61] We would like to point out that a different convention was employed in [27].
- [62] D. W. Oxtoby, “Vibrational population relaxation in liquids,” in *Advances in Chemical Physics* (John Wiley and Sons, Inc., 2007) pp. 487–519, ISBN 9780470142660
- [63] B. P. Krueger, G. D. Scholes, and G. R. Fleming, *J. Phys. Chem. B* **102**, 5378 (1998)
- [64] G. D. Scholes, C. Curutchet, B. Mennucci, R. Cammi, and J. Tomasi, *J. Phys. Chem. B* **111**, 6978 (2007)
- [65] J. Neugebauer, C. Curutchet, A. Muñoz Losa, and B. Mennucci, *Journal of Chemical Theory and Computation* **6**, 1843 (2010)

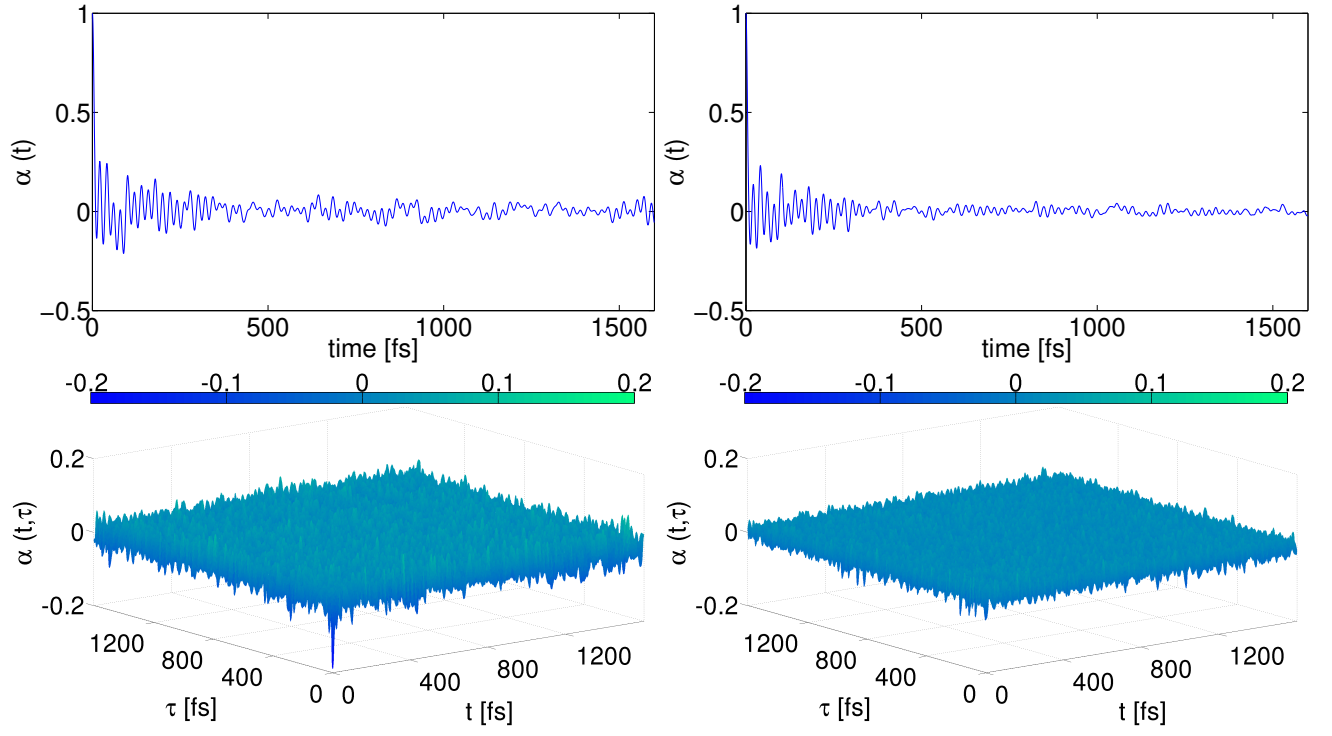


Figure 10. Same as for Fig. 8 but for site 2 of the FMO complex.

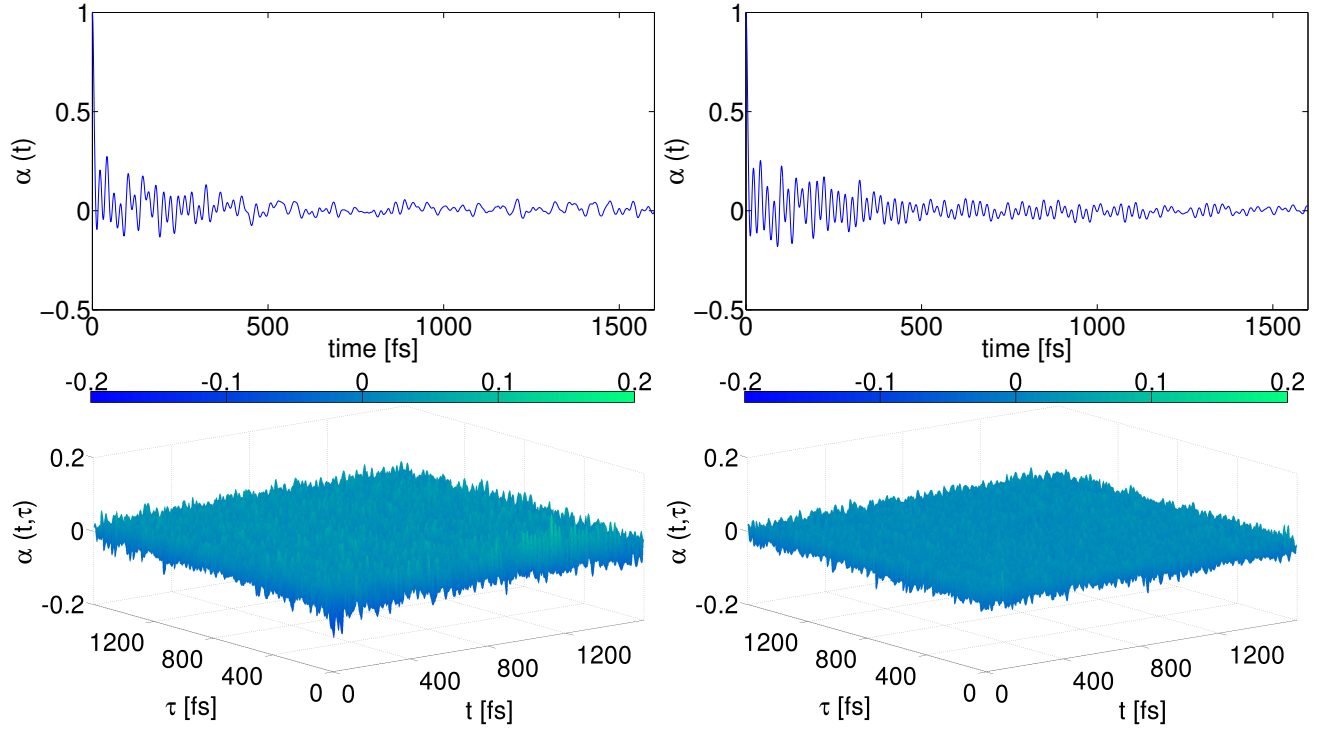


Figure 11. Same as for Fig. 8 but for site 2 of the FMO complex.

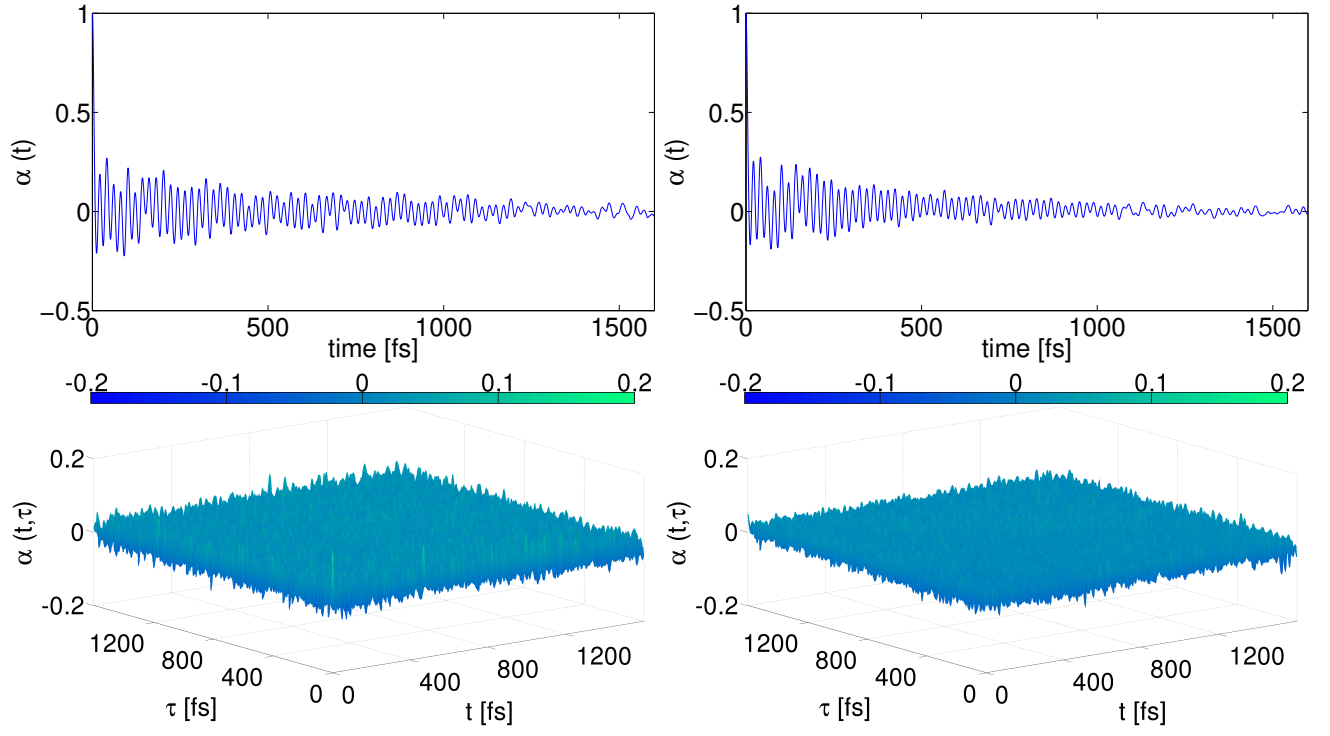


Figure 12. Same as for Fig. 8 but for site 2 of the FMO complex.

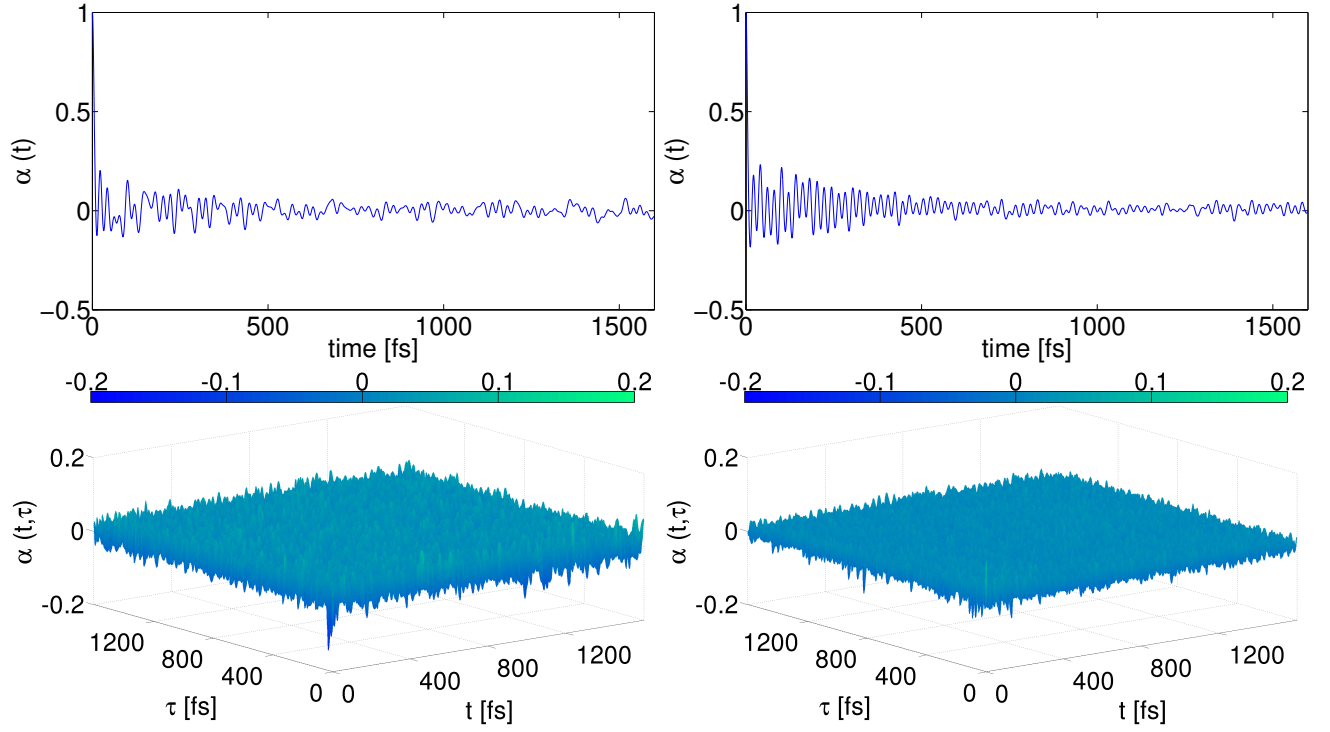


Figure 13. Same as for Fig. 8 but for site 2 of the FMO complex.

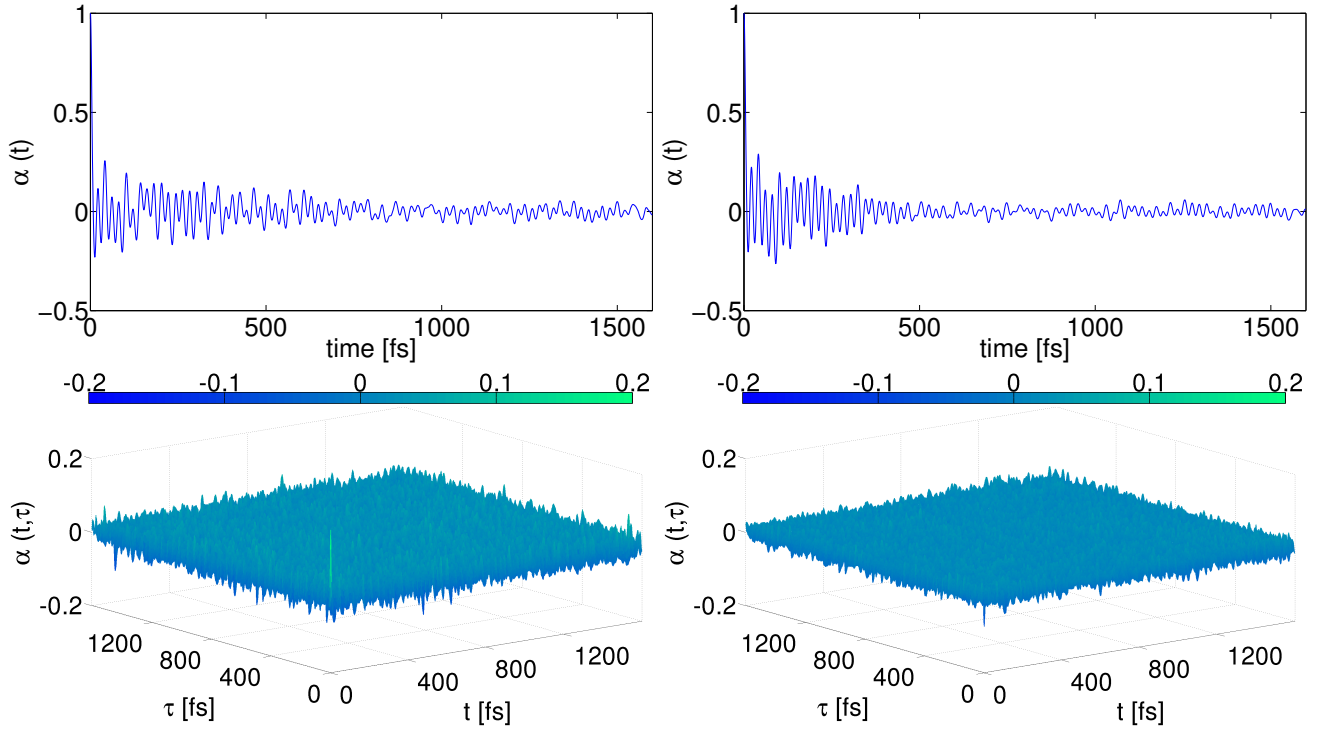


Figure 14. Same as for Fig. 8 but for site 2 of the FMO complex.

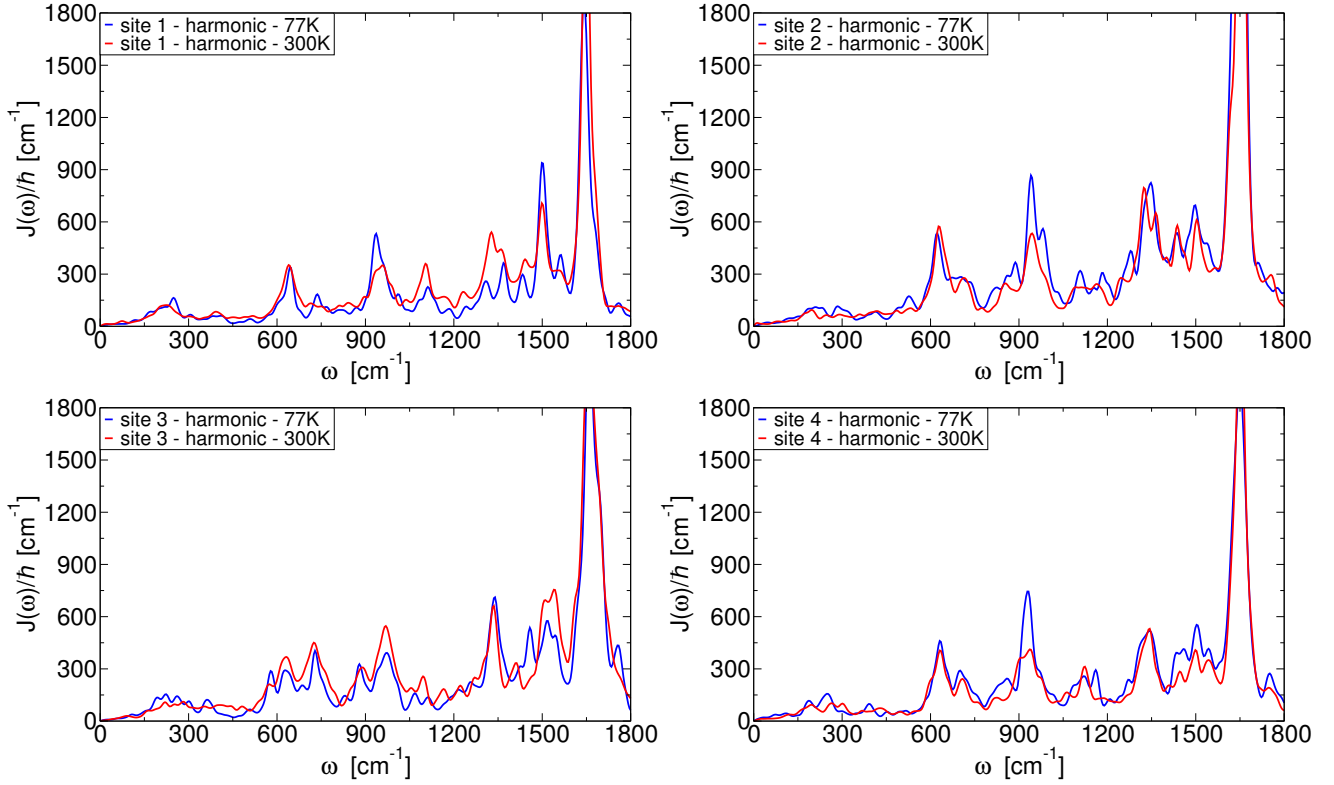


Figure 15. Comparison of the asymmetric component of temperature-dependent coupling density $G_{\text{asym}}(\omega) = J(\omega)$; for sites 1-4 of the Fenna-Matthews-Olson complex, obtained with the Harmonic approximation (As described in the text) at 77K and at 300K. Note that, as described in the text, the spectral density can be obtained by dividing $J(\omega)$ by 2π .

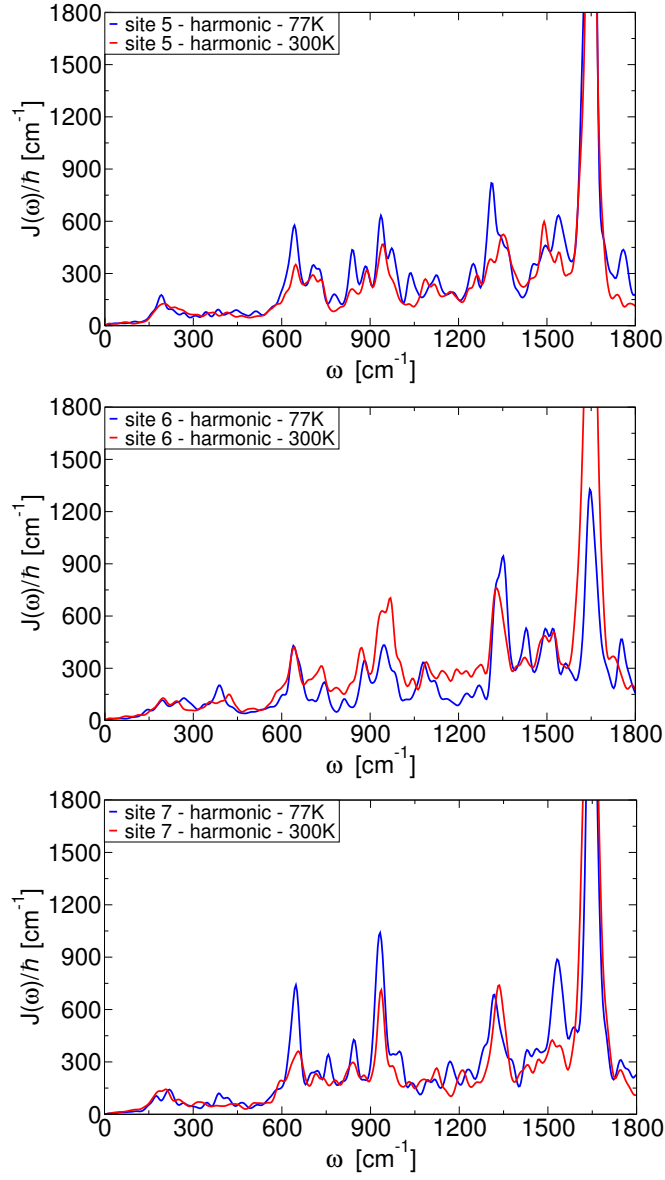


Figure 16. Comparison of the asymmetric component of temperature-dependent coupling density $G_{\text{asym}}(\omega) = J(\omega)$; for sites 5-7 of the Fenna-Matthews-Olson complex, obtained with the Harmonic approximation (As described in the text) at 77K and at 300K. Note that, as described in the text, the spectral density can be obtained by dividing $J(\omega)$ by 2π .